

DYNAMIC IMPLICATIONS OF  
BAJA CALIFORNIA MICROPLATE  
KINEMATICS ON THE  
NORTH AMERICA – PACIFIC PLATE  
BOUNDARY REGION

Dissertation

zur Erlangung des Doktorgrades  
der Fakultät für Geowissenschaften der  
Ludwig-Maximilians-Universität München

vorgelegt von Christina Plattner

am 2. März 2009

1. Gutachter: Prof. Rocco Malservisi
  2. Gutachter: Prof. Dr. Hans-Peter Bunge
- Tag der mündlichen Prüfung: 03.07.2009

## EHRENWÖRTLICHE VERSICHERUNG

Ich versichere hiermit ehrenwörtlich, dass die Dissertation von mir selbständig, ohne Beihilfe angefertigt worden ist.

München, den 2. März 2009

## ERKLÄRUNG

Hiermit erkläre ich, dass die Dissertation noch nicht in einem anderen Prüfungsverfahren vorgelegt und bewertet wurde.

Hiermit erkläre ich, dass ich mich anderweitig einer Doktorprüfung ohne Erfolg **nicht** unterzogen habe.

München, den 2. März, 2009

## ACKNOWLEDGEMENTS

Financial support for this work came from Deutsche Forschungsgemeinschaft (DFG) and the International Graduate School THESIS of the Elitenetzwerk Bayern.

I thank the geodynamics group at Ludwig-Maximilians-Universität for providing the framework of this thesis, in particular Prof. Peter Bunge, Dr. Helen Pfuhl, and IN SPECIFIC MY ADVISOR PROF. ROCCO MALSERVISI. I want to thank all international collaborators of the DFG project, and coauthors of publications resulting from this work: Dr. Rob Govers, Prof. Kevin Furlong, Prof. Tim Dixon, Prof. Paul Umhoefer, Dr. Francisco Suarez-Vidal, and others.

I want to acknowledge all the people that have been supporting my forthcoming during the last years in different ways, including many colleagues within the Department of Earth and Environmental Sciences at LMU, my internal and external mentors from LMU Mentoring Geosciences, Prof. Bettina Reichenbacher and Dr. Oliver Heidbach, and in particular MY FAMILY AND FRIENDS.

# TABLE OF CONTENTS

ABSTRACT.....	7
1. Extended Summary .....	8
Plate boundary deformation .....	8
Tectonic history of the North America – Pacific plate boundary region and Baja California .....	12
Kinematics of Baja California.....	15
Dynamics of Baja California microplate transport.....	17
Dynamic implications of microplate motion on the western North America plate boundary evolution .....	19
2. New constraints on relative motion between the Pacific plate and Baja California microplate (Mexico) from GPS measurements .....	22
Abstract .....	22
Introduction.....	23
Data Analysis .....	25
Stable Pacific plate reference frame.....	28
Rigidity of the Baja California microplate.....	34
Pacific - Baja California motion.....	39
North America - Pacific motion .....	42
Discussion .....	47
Acknowledgements .....	48
3. On the plate boundary forces that drive and resist Baja California .....	49
Abstract .....	49
Introduction.....	49
Model setup.....	51
Modeling results .....	54

Plate coupling on geodetic timescales.....	54
Plate coupling on geologic timescales.....	58
Model sensitivity.....	60
Analysis.....	61
Discussion and conclusions.....	63
Acknowledgements.....	64
4. Development of the Eastern California Shear Zone: Effect of pre-existing weakness in the Basin and Range?.....	65
Abstract.....	65
Introduction.....	66
Model description.....	68
Model results.....	71
Response to Baja California microplate motion.....	74
Response to Sierra Nevada microplate motion.....	75
Model sensitivity.....	77
Analysis.....	80
Conclusions.....	81
5. CONCLUSIONS.....	82
6. References.....	85
7. Appendix A: Preliminary velocity field in central BAJA.....	96
8. Appendix B: Coupling stresses at the PAC - BAJA plate boundary.....	97
B.1 Plate motion partitioning across NAM – PAC in dependency on the stress magnitude.....	97
B.2 Influence of incomplete decoupling in the Gulf of California.....	98
B.3 Temporal evolution of PAC – BAJA coupling.....	100

## **ABSTRACT**

Many plate boundaries appear to be broad deformation zones, composed of several smaller microplates (e.g. California, Alaska, Mediterranean sea). To accurately address plate boundary deformation, as needed for seismic hazard assessment, it is important to study the motion of these microplates. Furthermore the dynamics of microplates, such as their driving forces and the implication of their motion on the surrounding plate boundary region are not well understood. Following suggestions from previous studies that Baja California is a microplate located within the North America – Pacific plate boundary region, a kinematic study using horizontal velocity data from Global Positioning System was performed. Building on the kinematic results and using numerical modelling techniques, a 2D mechanical model that simulates the transport of the Baja California microplate by lithospheric coupling with the Pacific plate was created. This model addresses the transport forces, and necessary preconditions in the North America – Pacific plate boundary region for rigid microplate transport. In addition, this model provides insights on the deformational response of western North America to Baja California motion, in particular the kinematic response of neighbouring microplates and the activation of passive fault systems. This latter was examined in more detail by separating the contribution of deformation from Baja California microplate motion and Sierra Nevada microplate motion to the formation of the Eastern California Shear Zone. Overall, it was found, that microplates play an important role for plate boundary kinematics and that their motion strongly influences the dynamics and fault evolution in plate boundary regions.

# 1. Extended Summary

## Plate boundary deformation

Plate tectonics theory describes that the lithosphere is divided into nearly rigid plates that move with respect to each other. The rigidity of the plates allows for stresses to transmit over large areas, while the deformation is restricted to narrow regions at the plate boundaries. This localized deformation explains the first order observation of the global earthquake distribution, volcanoes, and orogenic belts along plate boundaries (Figure 1.1). However, a closer examination of the seismicity distribution and topography shows that plate boundaries can be accommodated in broader regions. This is particularly true for continental plate boundaries (Kearey et al, 2009).

Space geodetic measurements have substantially increased the spatial resolution of the surface velocity field during the last decades. Particularly in plate boundary regions on the continents, an accurate Euler pole description of these motions called for an increasing amount of plate elements, so-called microplates (McCaffrey, 2002; Thatcher, 1995).



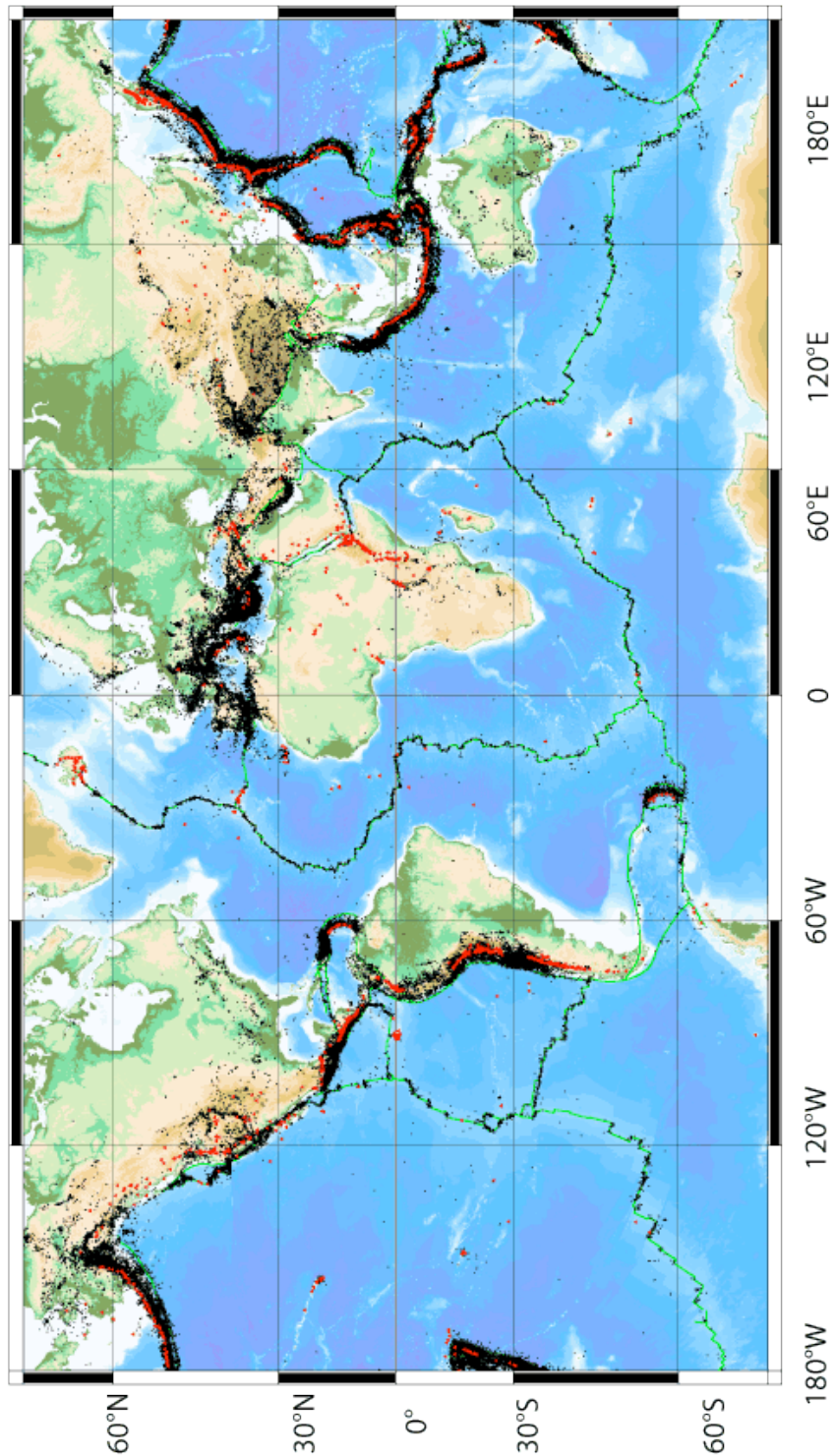


Figure 1.1: Orogenic belts (Global topography and bathymetry from General Bathymetric Chart of the Oceans, GEBCO, 2004), distribution of earthquakes (shown as black dots, data from 2000-2008, National Earthquake Information Center), and volcanoes (shown as red triangles, data from Smithsonian) are clustered along plate boundaries outlining the rigid plates.

With this subdivision, the word “plate” has started to lose its meaning as an individual mechanical entity for which concepts such as torque balance (Forsyth and Uyeda, 1975) make sense. In the classical view, the motion and dynamics of a plate could be understood from body forces, coupling of the plates to the asthenosphere, and interaction of plates along their boundaries. Even the relatively small Juan de Fuca plate is driven entirely from within (Govers and Meijer, 2001). In contrast, it is commonly assumed that microplates are externally driven, i.e. their motion is only a response to the dynamics of their neighboring plates and frictional forces along the microplate boundaries. Since microplates can be features that live longer than instantaneous, their presence and dynamics must play an important role for the plate boundary evolution.

The North America (NAM) – Pacific (PAC) plate boundary is a typical example of a broad deformation region. Assuming earthquakes are a proxy for deformation, then it can be seen that the plate boundary is diffuse from the Colorado plateau (approximately 100°W) to the Pacific coast (Figure 1.2) with smaller rigid microplates such as the Sierra Nevada (SIERRA) and Baja California (BAJA) around which the earthquakes cluster (Figure 1.2). The aim of this thesis is to assess the dynamics driving these microplates (in particular BAJA), and the dynamic consequences of the microplate motions on the surrounding plate boundary region.

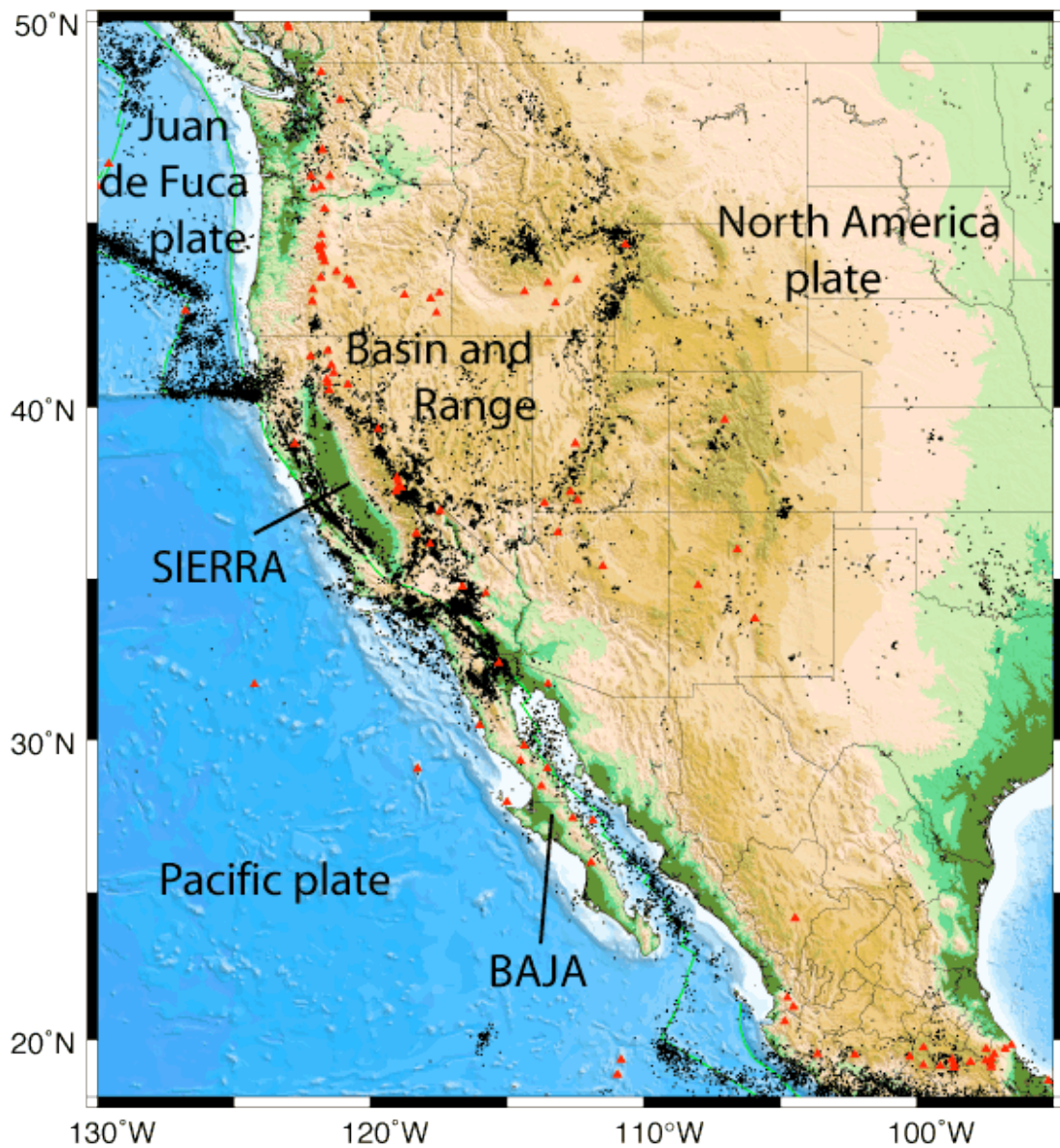


Figure 1.2: The topography, distribution of earthquakes, and volcanoes (for data source see Fig. 1.1.) reveal that the North America - Pacific (NAM – PAC) plate boundary is a broad and diffuse deformation zone composed of multiple smaller nearly rigid plates (microplates) bounded by narrow deformation zones. The Sierra Nevada (SIERRA) and Baja California (BAJA), are examples of fault-bounded microplates located within the NAM – PAC plate boundary region. In contrast the Basin and Range area is a diffuse deformation zone, though still bounded by more active regions in the east and west.

## **Tectonic history of the North America – Pacific plate boundary region and Baja California**

Until about 30 Ma the Farallon (FA) plate was subducting along the western NAM margin and Baja California was still part of the NAM plate (Figure 1.3 A). Since the subduction rate of the FA plate was faster than the mid-ocean ridge spreading rate between FA and PAC, the ridge approached the NAM trench. Following the ridge subduction, a transform fault initiated at the NAM - PAC plate boundary (Figure 1.3 B). With the ongoing subduction of the Farallon – PAC ridge, and the migration of the two bounding triple junctions in opposite directions this new plate boundary grew (Atwater, 1998).

While the majority of the ridges along the NAM margin were completely subducted, this was not the case along BAJA. At first, the FA plate broke up into smaller oceanic microplates (Figure 1.4 A). Then the spreading center between these oceanic microplates and the PAC plate approached the NAM trench. Subsequent the young oceanic material became too buoyant to be subducted (Nicholson et al., 1994). The oceanic microplates started to become more and more coupled with the overriding plate, leading to the cessation of subduction and the cessation of the spreading at the remaining mid ocean ridges. In response, the continental margin widened and the plate boundary migrated eastward into the so-called Protogulf, an extensional area, like the Basin and Range area in western NAM (Figure 1.4 B) (Stock and Hodges 1989). As this plate boundary localized in the Gulf of California, where seafloor spreading started approximately at 6 Ma in the south, BAJA was detached from mainland Mexico (NAM) and translated with the PAC plate (Figure 1.3 C; Figure 1.4 C) (Atwater, 1998; Stock and Hodges, 1989; Umhoefer 1997).

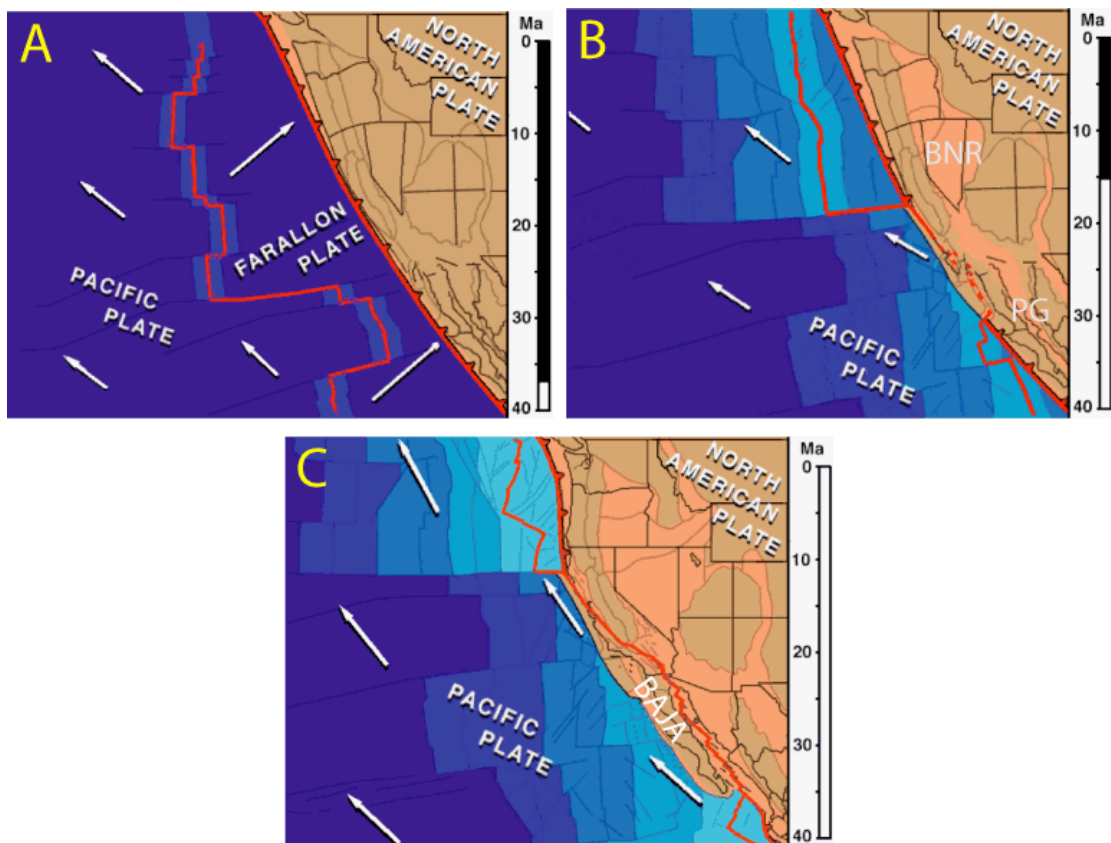


Figure 1.3: Tectonic history of the North America (NAM) – Pacific (PAC) plate boundary. Figures from tectonic animation of T. Atwater, following Atwater and Stock (1998). A) Seafloor spreading between Pacific (PAC) and Farallon plates (FA), subduction of FA under NAM. B) Initiation of NAM – PAC plate boundary, east-west extension in the Basin and Range area (BNR) and the Protogulf (PG) (both indicated by dark shaded areas) and brake-up of the Farallon plate. C) Inland migration of the main plate boundary, formation of the Gulf of California and rupture of Baja California (BAJA) from NAM.



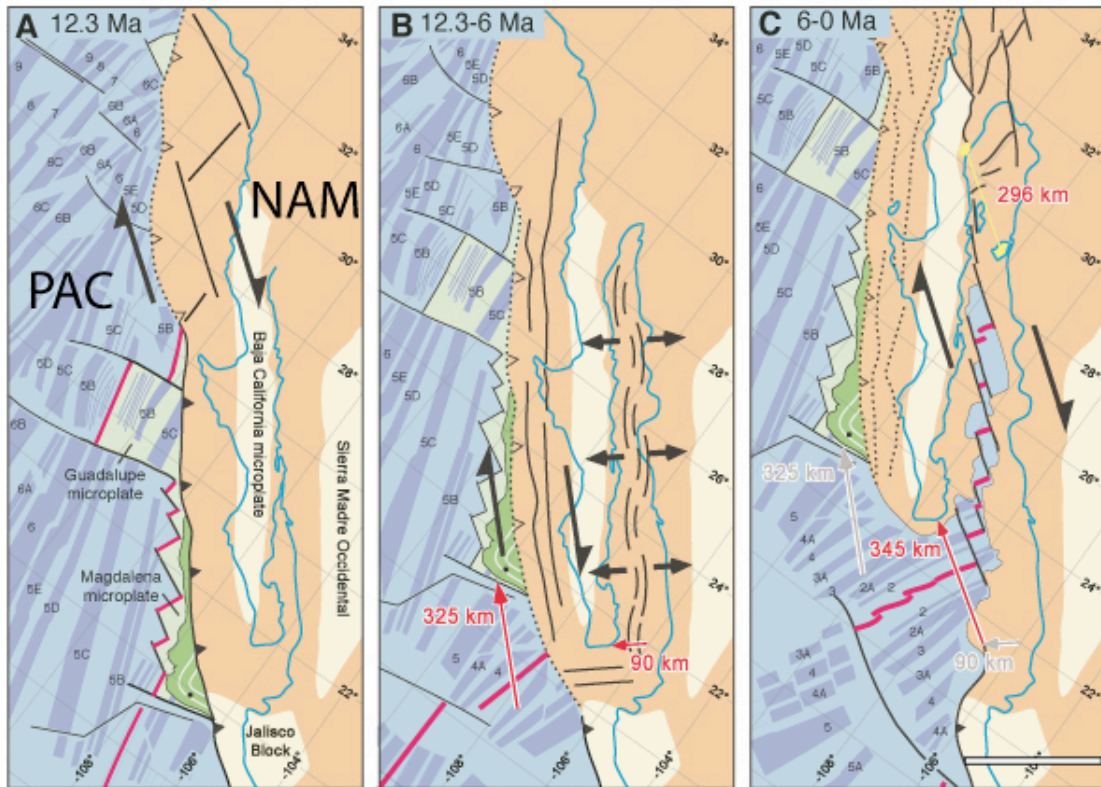


Figure 1.4: Tectonic history of Baja California (BAJA) (Figure from Fletcher et al., 2007). A) 12.3 Ma: BAJA is still part of the NAM plate. In the south: Subduction of the microplates remaining from the Farallon plate brake-up. In the north: Initiation of the strike-slip plate boundary between the North America (NAM) and Pacific (PAC) plates. B) 12-6 Ma: Coupling between PAC – BAJA led to distributed extension (mainly east – west) in the Protogulf. Along the continental margin mainly north – south directed strike-slip faulting, for which Fletcher et al. (2007) suggested higher rates than for the present-day strike-slip faulting west of BAJA. C) After 6 Ma the main plate boundary localized in the Gulf of California (east of BAJA) as a transensional fault system with sea-floor spreading observed in the southern Gulf of California.

It has been a common assumption that since 6 Ma BAJA has been part of the stable PAC plate. However, recently, geological and geodetic observations suggested that some differential motion between PAC and BAJA exists (Michaud et al., 1994; Dixon et al., 2000, Gonzalez-Garcia et al., 2003). To assess and quantify this differential motion, a kinematic study was performed. This kinematic information is also the basis for following geodynamic studies such as testing theories on microplate driving forces, and on the dynamic implications of microplate motion on the plate boundary evolution.

### **Kinematics of Baja California**

In the past decades the precision of satellite based geodetic measurements, such as from Global Positioning System (GPS) has steadily increased, making the use of horizontal velocities from GPS appropriate for plate motion studies (Dixon, 1991). The available GPS surface velocity field from BAJA was used to show that BAJA is a microplate, and to quantify its rigidity (internal deformation) and its relative motion with respect to the neighboring plates (Plattner et al., 2007, see here chapter 2).

To compare the motion of BAJA to its neighboring plates, it was necessary to quantify the rigid plate rotations of the NAM and PAC plates (as defined by an Euler vector). The rotation of the stable NAM plate has been subject to previous studies by different authors. Here the stable NAM plate rotation by Sella et al. (2006) was adopted. On the other hand, only a few studies existed for the PAC plate and GPS sites are scarce there (limited to oceanic islands). As the relative motion between BAJA and the PAC plate depends directly on the stable PAC plate rotation, a more detailed study was performed. A new

Euler vector describing the stable PAC plate rotation was established, incorporating new GPS velocity data from a sea-level monitoring project. Statistical tests on the model sensitivity to the GPS stations were performed to identify outliers. A F-test was used to verify that this PAC plate motion model had a significantly lower misfit without BAJA being part of this plate, compared to having BAJA as a part of PAC (Plattner et al., 2007; see here chapter 2).

Euler vector calculations were also performed to quantify the rigid BAJA microplate rotation, and to address the regional extent of rigid BAJA (identifying the deformation zones). These calculations included tests for elastic strain accumulation from the microplate bounding faults to bias the GPS velocity data (McCaffrey, 2002). It was found that, in agreement with geological studies the microplates border is marked by known fault traces (Figure 2.1) (Allan et al., 1960; Michaud et al., 2004; Busch et al., 2006; Fletcher et al., 2007). The residual motion within rigid BAJA showed an average velocity of 1.5 mm/yr. Although all residuals were within the GPS uncertainty, their azimuth was not randomly distributed, which should be the case if they were only related to measurement uncertainties (Figure 2.4). An upper bound of the internal deformation ( $-1 \times 10^{-16} \text{ sec}^{-1}$ ) could be asserted by assuming that the observed relative motion between the northern and southern network is significant. Preliminary velocity data from central BAJA could not yet provide information on the accommodation of this strain (Appendix A).

The NAM, PAC, and BAJA Euler vectors were combined to allow the determination of rigid plate relative motions at any point of a common boundary between two plates. The comparable location of NAM – PAC and



NAM – BAJA rotation poles showed that BAJA is moving in the same direction as the PAC plate with respect to stable NAM. The rotation rates showed a 10% slower NAM – BAJA relative motion compared with NAM - PAC. This kinematics suggest partial coupling between the PAC plate and BAJA microplate. The plate relative motion between PAC and BAJA calculated for the common plate boundary is in agreement with rates from previous geologic studies at this location (Michaud et al., 2004; Fletcher et al., 2007). The geodetic NAM – BAJA Euler vector agrees with the Euler vector of the geologic model NUVEL-1A (DeMets et al., 1994), for which seafloor-spreading rates from the Gulf of California were used (with the intention to represent NAM – PAC motion, as it was believed that BAJA is part of the stable PAC plate). In comparison the geodetic NAM – PAC Euler vector agrees with a geologic NAM – PAC Euler vector from a model that excludes the Gulf of California (DeMets, 1995). The similar geodetic and geologic rates suggest that the plate relative motions between all three plates were constant during the last 3 Myrs, the time period sampled in the geologic models (Plattner et al., 2007; see here chapter 2).

### **Dynamics of Baja California microplate transport**

The kinematics results suggested partial coupling between BAJA and PAC plate. This agrees with the hypothesis of Nicholson et al. (1994), that the rupture of BAJA was initiated by lithospheric coupling along the present-day BAJA - PAC plate boundary. Following this idea, the dynamics of such mechanical coupling as a driving force for BAJA were tested (Plattner et al., 2009, see here chapter 3). A 2D spherical cap model was created that simulates the rigid plate rotation of PAC with respect to a fixed NAM plate.

The BAJA microplate was included in the model geometry and the relative motions at the plate boundaries adjacent to BAJA observed. Mechanical coupling between PAC and BAJA was simulated by differential shear stresses along this plate boundary. For different mechanical coupling the plate motion partitioning between PAC – BAJA and BAJA - NAM was calculated (Appendix B.1). The stress magnitude necessary to fit the geodetic rigid plate relative motions was quantified by calibrating the plate motion partitioning.

To the north the model geometry extended as far as the SIERRA microplate, allowing to observed the kinematic response to BAJA in this region. The model was validated using the geodetic rigid SIERRA microplate motion (Psencik et al., 2006) and neotectonic fault slip rates in the BAJA – NAM collision zone (as summarized in Becker et al., 2005). These kinematic observations from the model also showed that BAJA as a moving microplate has the potential to reactivate normal faults in the western Basin and Range area as strike-slip faults (see also chapter 4).

To test the dynamics during the Protogulf, when BAJA was still coupled to NAM but starting to move northward (approximately at 6 Ma), simultaneous mechanical coupling was applied along the BAJA – NAM plate boundary. It could be shown that coupling stresses must have been already low at that time in order to allow BAJA to move as a rigid block (Appendix B.2).

The model geometry was changed to represent the plate boundary configuration at 3 Ma, when some of the major shear zones in the BAJA – NAM collision zone were not yet formed. Without these shear zones resisting forces in western NAM were higher and the coupling stresses of 10 MPa were too low in order to drive BAJA at the observed rate with respect to NAM. For

constant plate motions during the last 3 Ma, thus, the coupling stresses needed to be higher in the past (Appendix B.3). A possible explanation for the decrease of coupling stresses with time can be a decrease in buoyancy due to cooling of the subducted slabs under BAJA during the last 12 Myrs.

### **Dynamic implications of microplate motion on the western North America plate boundary evolution**

In the previous chapter it was shown that BAJA motion affects the kinematics in western NAM. The motion of microplates can lead to the evolution of large fault zones in plate boundary regions. The Eastern California Shear Zone (ECSZ) in western NAM is a prime example of a shear zone within a plate boundary regime bordered by microplates (Figure 1.5). It has been proposed that this shear zone formed as a result of the northward propagation of the Gulf of California shear (McCroory et al., 2009; Harry, 2005; Faulds et al., 2005), i.e. northward motion of BAJA.

However, fault ages partially contradict simple northward propagation of shear strain and suggest that shear in the ECSZ localized prior to BAJA motion (Oskin and Iriondo, 2004; Miller and Yount, 2002, McQuarrie and Wernicke, 2005; Reheis and Sawyer, 1997). As the ECSZ is also the eastern boundary of the Sierra Nevada microplate (SIERRA), this model of ECSZ genesis implies, that the SIERRA microplate formed after, and as a result of BAJA motion.

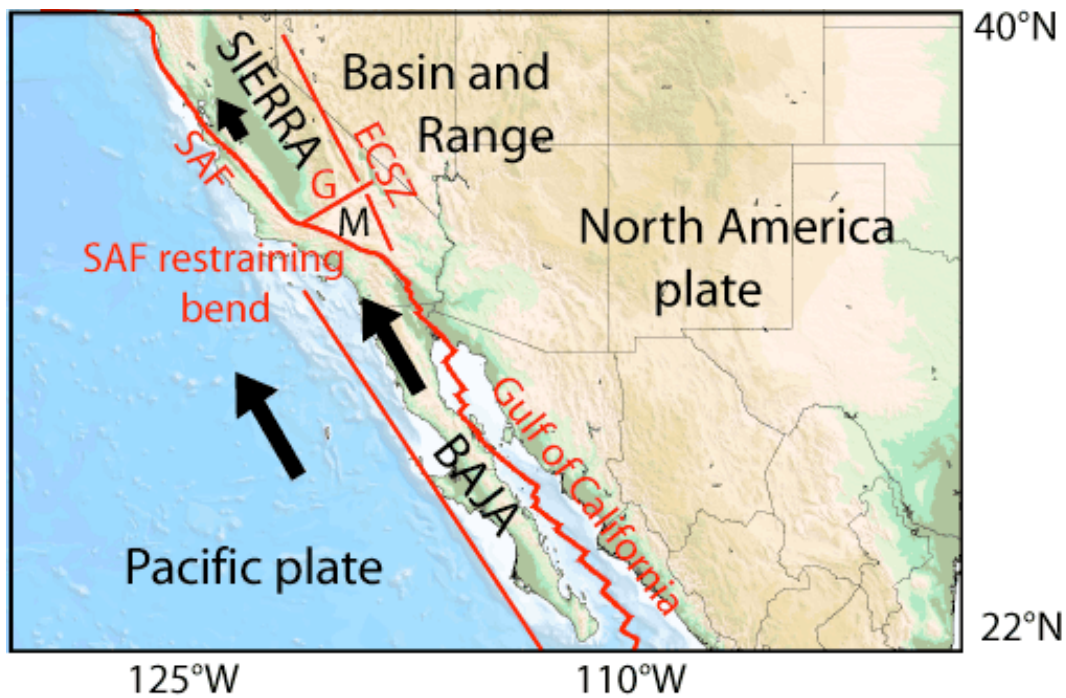


Figure 1.5: Microplates and microplate boundaries in the North America – Pacific plate boundary region: Sierra Nevada microplate (SIERRA), Baja California microplate (BAJA), Mojave block (M), San Andreas Fault (SAF), Eastern California Shear Zone (ECSZ), Garlock Fault (G). Black arrows indicate the plate motion direction with respect to fixed North America.

As much of the tectonic evolution of SIERRA is similar to the one of BAJA, similar driving forces may have existed in the past. Additionally, since the SAF is older than BAJA, driving forces at SIERRA could have started earlier, better agreeing with the geological data on shear initiation at the ECSZ. Still, even assuming larger coupling early in the history, the formation of a distinct shear zone about 150 km inland from the SAF cannot be explained only from dragging of the SIERRA along the SAF. A numerical model was created to test under which conditions high shear strain develops along the ECSZ from dragging of SIERRA along the SAF. In particular, the effect of pre-existing weakness in the Basin and Range was tested, as justified by the middle Miocene extension that thinned and weakened the lithosphere. The model showed that this pre-existing weakness has a major effect on the strain

pattern in western NAM. Analysis of the shear strain pattern in the models suggested that the northern ECSZ develops at the SIERRA batholith – Basin and Range border along the mechanical weakness when shear is applied to the western SIERRA (along the SAF). In contrary, without such a weakness, strain does not concentrate in the ECSZ. This shows that pre-existing weaknesses play an important role in the present-day strain accommodation and in the plate boundary evolution.

A consequence of the formation of the ECSZ prior to the beginning northward motion of BAJA is, that resisting forces for BAJA motion in western NAM were low from early on. Furthermore, it was found that SIERRA microplate motion implies shear deformation in the Protogulf associated with a relative motion of about 5 mm/yr between BAJA and NAM (about 10% of the present-day shear). These results show that the formation and motion of microplates in broad plate boundary regions are highly interactive. Tectonic studies in such plate boundary regime should therefore consider the kinematics of the adjacent microplates.

## **2. New constraints on relative motion between the Pacific plate and Baja California microplate (Mexico) from GPS measurements<sup>1</sup>**

### **Abstract**

We present a new surface velocity field for Baja California using GPS which we use to test the rigidity of this microplate, calculate its motion in a global reference frame, determine its relative motion with respect to North America and the Pacific, and compare those results to our estimate for Pacific – North America motion. Determination of Pacific plate motion is improved by the inclusion of four sites from the South Pacific Sea Level and Climate Monitoring Project. These analyses reveal that Baja California moves as a quasi-rigid block with respect to the Pacific plate, and is moving in the same direction, but at a slower rate, than the Pacific plate relative to North America. This is consistent with seismic activity along the western edge of Baja California (the Baja California shear zone), and may reflect resistance to motion of the eastern edge of the Pacific plate caused by the “big bend” of the San Andreas fault and the Transverse Ranges in southern California.

---

<sup>1</sup> This chapter has been published as: Plattner, C., Malservisi, R., Dixon, T.H., LaFemina, P., Sella, G.F., Fletcher, J., and Suarez-Vidal, F., 2007, New constraints on relative motion between the Pacific Plate and Baja California microplate (Mexico) from GPS measurements: *Geophysical Journal International*, v. 170, p. 1373-1380.

## Introduction

Plate rigidity is a key assumption in plate tectonics. While this assumption works well for plate interiors, plate boundaries can include a broad region of deformation and the development of multiple blocks or “microplates”. This is particularly true for the Pacific – North American plate boundary (e.g. Atwater and Stock, 1988). Identifying these rigid blocks provides important kinematic boundary conditions for tectonic studies of western North America.

Constraints on North America - Pacific plate motion are also important for kinematic tectonic studies of western North America and parts of the circum-Pacific region. Models of this motion on geologic time-scales (e.g., DeMets et al., 1990; 1994) may use magnetic anomalies from the spreading centre in the southern Gulf of California. However, evidence is accumulating that Baja California’s motion is distinct from that of the Pacific plate (Figure 2.1) and thus behaves as a separate block or microplate (Dixon et al., 2000b; Fletcher and Munguia, 2000; Gonzalez-Garcia et al., 2003; Michaud et al., 2004). Here we use new GPS data to quantify current North America – Pacific plate motion and investigate coupling and rigidity of Baja California and the Pacific plate.

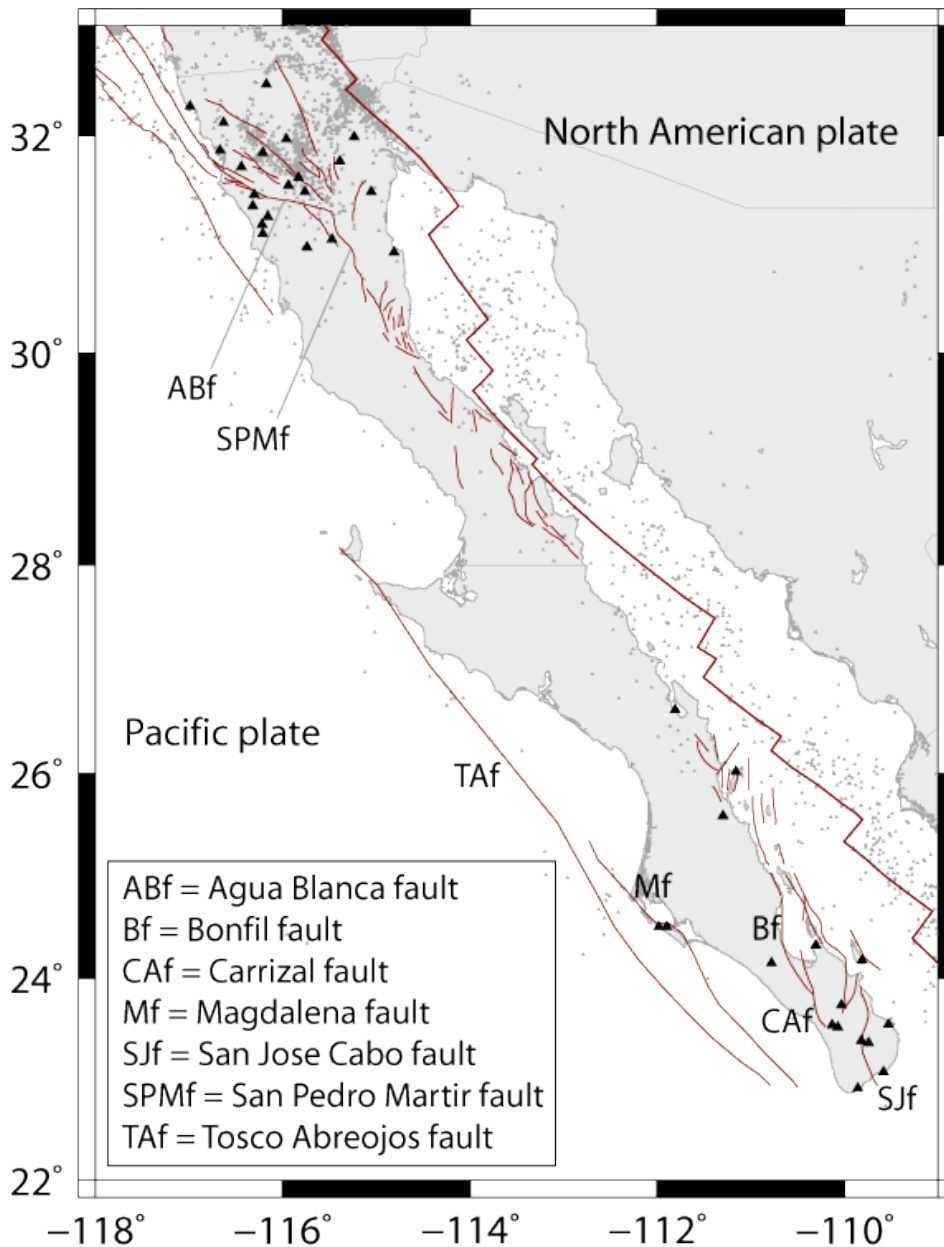


Figure 2.1: Baja California, Mexico: Faults above latitude 28 from Instituto Nacional Estadística Geografía e Informática de México and Dixon et al. (2002), faults south of latitude 28 by Paul Umhoefer (personal communication) and Michaud (2004). Epicenters from National Earthquake Center Information (1973 to present). The geologically defined rigid block is outlined by Agua Blanca fault (ABf), San Pedro Martir fault (SPMf), San Jose del Cabo fault (SJf), Bonfil fault (Bf) and Carrizal fault (CAf), Tosco Abreojos fault (TAf), Magdalena fault (Maf).



## Data Analysis

For the Pacific plate we use only continuous GPS (CGPS) with time series longer than three years, giving time-series durations from three to ten years (Table 1). Compared to previous studies of Pacific plate motion we add four new sites from the South Pacific Sea Level and Climate Monitoring Project (SPSLCMP) improving kinematic constraints in the central and western Pacific. To reduce the uncertainty in the time-series of GUAX on Guadalupe Island, we added episodic GPS (EGPS) data from GAIR through a vector tie (Sella et al. 2002), which extends the time-series back to 1993. The uncertainty of this new time-series, here called GUAZ, is reduced by 40%, while the velocity changes only by 0.1 mm/yr in all 3 components.

32 of 33 GPS stations in Baja California are episodic GPS (EGPS) sites. We use EGPS data from sites with at least three occupation episodes of two and more 24hr days and a minimum total time span of 6 years since 1993. We did not use data from before 1993 due to incomplete orbit information.

All data were processed using GIPSY/OASIS II, Release 5.0 software and non-fiducial satellite orbit and clock files provided by the Jet Propulsion Laboratory (Zumberge et al. 1997). The data analysis follows Sella et al. (2002), but the daily solutions are aligned to IGB00 (Ray et al. 2004). The velocity and its uncertainty for each site are then calculated by linear regression. Outliers with an offset of more than 3 times the formal error are not considered in the regression. Velocity uncertainties are calculated following Mao et al. (1999) and Dixon et al. (2000a).

We calculate the stable plate reference frames for Pacific and Baja California

by the best fitting Euler vector (Ward, 1990; Minster et al., 1974), testing for plate rigidity by comparing velocity residuals to uncertainties. Using the stable North America reference frame of Sella et al. (2006) we calculate its relative plate motion with the Pacific plate and Baja California microplate.

Table 1: GPS data used for the computation of Pacific Euler vector and their residual rate.

Site id*	Lon. (°E)	Lat. (°N)	$\Delta T$ yea	IGb00			Residual to PA1***			PA1 Importance (%)	
				Ve mm/yr	$\sigma_{Ve}$ ** mm/yr	Vn mm/y	$\sigma_{Vn}$ ** mm/yr	Rate mm/y	$\sigma_{ra}$ ** mm/y		Azi. (°) ***
chat <sup>1</sup>	-176.57	-43.96	10	-41.2	0.3	32.3	0.3	1.0	0.5	78	-
CKIS <sup>2</sup>	-159.80	-21.20	4	-63.5	0.8	33.8	0.5	0.4	0.7	-46	13
guaz <sup>4</sup>	-118.29	28.88	12	-47.7	0.3	23.4	0.3	2.0	0.6	149	-
hnlc <sup>1</sup>	-157.86	21.30	5	-63.6	0.8	33.8	0.6	0.9	0.9	-71	-
KIRI <sup>2</sup>	172.92	1.35	3	-67.10	1.1	30.7	0.6	1.4	1.0	50	8
KOK1 <sup>1</sup>	-159.76	21.98	7	-63.0	0.6	33.8	0.4	0.3	0.5	-22	21
KWJ1	167.73	8.72	6	-69.7	0.7	27.7	0.4	0.6	0.5	176	10
MARC <sup>3</sup>	153.98	24.29	5	-73.3	1.4	21.5	1.2	2.3	1.4	-138	5
maui <sup>1</sup>	-156.26	20.71	7	-63.3	0.4	32.8	0.3	0.9	0.4	-142	-
mkea <sup>1</sup>	-155.46	19.80	9	-63.7	0.4	33.4	0.3	0.7	0.5	-96	-
POHN <sup>2</sup>	158.21	6.96	4	-70.2	1.3	26.5	0.8	1.6	0.9	-7	7
THTI <sup>1</sup>	-149.61	-17.58	7	-66.6	0.8	32.6	0.4	0.5	0.6	-159	20
TRUK <sup>3</sup>	151.89	7.45	4	-72.0	1.6	22.5	0.9	1.5	1.6	-83	6
TUVA <sup>2</sup>	179.20	-8.53	4	-64.2	0.9	31.2	0.5	1.1	1.0	97	10

\*Only upper case sites are used to compute the Pacific Euler vector. <sup>1</sup> IGS, <sup>2</sup> SPSLCMP, <sup>3</sup> WING, <sup>4</sup> SCEC time-series has been tied using guax and gair.

\*\* Uncertainties are  $1 \sigma$ .

\*\*\* Velocity after removing rigid motion of the Pacific plate (PA1) from the IGb00 velocities at each site. See table 2 for angular velocity.

\*\*\*\* Azimuth is the angle of the rate residual in degrees clockwise from North.

### **Stable Pacific plate reference frame**

Using standard geological criteria for the definition of a stable plate (e.g. Sella et al., 2002) we initially identified 21 CGPS sites on the Pacific plate interior. We excluded FALE due to its location in a Subduction-Transform Edge Propagator (STEP) region (Govers and Wortel, 2005). FARB, KOKB, NAUR, PAMA, TAHI and UP01 are known to have technical problems or large uncertainties and are therefore excluded. We use only one station from the Hawaiian Islands to avoid an overconstraint; the station importance (Minster et al., 1974) would sum up to 48%. We choose KOK1 as it is located furthest from volcanic activity. However we include all Hawaiian Island stations to compare residuals with respect to the stable Pacific plate.

As the stable Pacific plate reference frame is based upon a limited number of GPS stations we test its sensitivity to each GPS station. Using a jackknife method we compute 11 rotation poles from the dataset of 11 GPS stations (Table 1), leaving out one station at a time. We compare the rotation pole locations and the corresponding average residual motion within the Pacific plate. For every model we apply the F-test (Stein and Gordon, 1984) to test whether we obtain significant improvement. We recognize the limitations of these tests, in the sense that our sample size is small, and the tests assume normal distribution. While the 2D-error ellipses for all rotation poles overlap at 95% confidence, however, at the level of one standard error, the solutions are sensitive to exclusion of stations GUAZ and CHAT (Figure 2.2, Table 2).

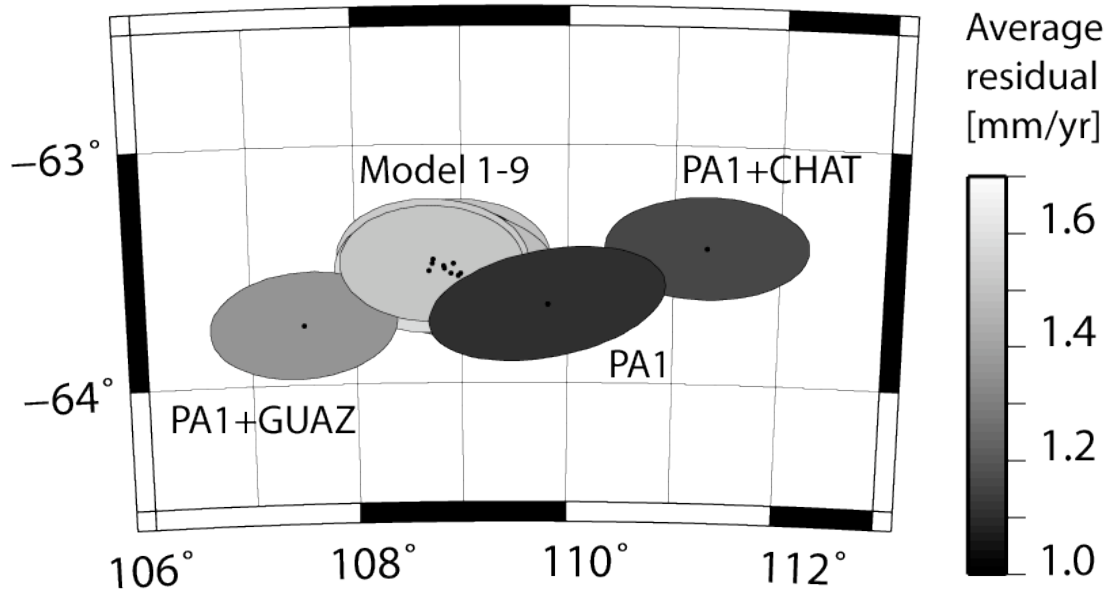


Figure 2.2: Stability of location of Pacific-IGb00 pole of rotation. Using 10 out of 11 stations we compute 11 rotation poles, leaving out 1 station at a time. The rotation pole shows increased sensitivity to GUAZ and CHAT. We exclude GUAZ and CHAT and use 9 stations (Table 1) to obtain our best-fitting pole of rotation. All rotation pole error ellipses are colour coded by the average residual motion, calculated from of the 11 stations plus HNLC, MKEA, and MAUI. For visibility only the 1 sigma error ellipses showing the 2D-error are shown.

Table 2: Pacific, North American and Baja California Euler vectors.

Rotation pole*	Lon. (°E)	Lat. (°N)	Omega (°/Myr)	$\sigma_{\max}$	$\sigma_{\min}$	Azi. (°)**	$\chi^2/DOF$
<i>Pacific plate – IGb00</i>							
PA1 (This study 9 stations***) – IGb00	109.81	-63.67	0.681±0.003	0.6	0.3	79	1.00
PA1 + GUAZ (10 stations) – IGb00	107.50	-63.75	0.677±0.003	0.4	0.3	86	1.62
PA1 + CHAT (10 stations) – IGb00	111.31	-63.43	0.679±0.003	0.5	0.2	90	1.47
<i>North America – IGb00</i>							
Sella et al., 2006	-83.82	-5.66	0.195±0.001	0.4	0.1	-1	
<i>North America – Pacific (geodetic)</i>							
Sella et al., 2006 – PA1	-75.89	50.16	0.769±0.004	0.5	0.3	-85	
Sella et al., 2006 – PA1 + GUAZ	-77.32	50.11	0.766±0.004	0.4	0.2	-87	
Sella et al., 2006 – PA1 + CHAT	-74.95	49.98	0.7680±0.004	0.5	0.2	77	
Beavan et al., 2002	-75.04	50.26	0.773 ± 0.004	0.4	0.2	94	
DeMets and Dixon, 1999	-73.70	51.50	0.765 ± 0.010	2.0	1.0	-85	
Gonzalez-Garcia et al., 2003	-77.01	49.89	0.766 ± 0.007	0.3	0.2	70	
Sella et al., 2002	-72.11	50.38	0.755 ± 0.007	0.6	0.4	-79	
<i>North America – Pacific (geologic)</i>							
NUVEL-1A (DeMets, 1994)	-78.2	48.7	0.749±0.012	1.3	1.2	-61	
<i>Baja California – IGb00</i>							
BAC1**** – IGb00	106.63	-64.73	0.637 ± 0.037	4.4	0.4	-53	3.50
<i>North America – Baja California</i>							
Sella et al., 2006 – BAC1	-78.11	50.16	0.725±0.039	3.14	0.4	62	

The first plate rotates counterclockwise relative to the second plate around the stated rotation pole.

\* Lengths in degrees of the semi-major axes sig maj and semi minor axes sig min of the 1 sigma pole error ellipse. Both axes are derived from a 2 dimensional error distribution.

\*\* Azimuth of the semi-major ellipse axis in degrees clockwise from north.

\*\*\* List of 9 sites used see Table 1.

\*\*\*\* List of 10 sites used see Table 3.

Angular velocity of PA1 relative to IGb00 in cartesian coordinates with covariance matrix. The X, Y, Z axes are parallel to (0°N,0°E), (0°N, 90°E), and (90°N), respectively.

Omega ( $10^{-3}$  rads/Myr): omegaX=-1.8186589 omegaY=4.9377246 omegaZ=-10.6312041

Covariance matrix ( $10^{-6}$  rads<sup>2</sup>/Myr<sup>2</sup>): xx=0.0064931 xy=0.0006229 xz=-0.0002533  
yy=0.0010012 yz=-0.0000000 zz=0.0026199

Angular velocity of BAC1 relative to IGb00 in cartesian coordinates with covariance matrix:

Omega ( $10^{-3}$  rads/Myr): omegaX=-1.3575097 omegaY=4.5444985 omegaZ=-10.0461015

Covariance matrix ( $10^{-6}$  rads<sup>2</sup>/Myr<sup>2</sup>): xx=0.0865653 xy=0.1960590 xz=-0.1088797  
yy=0.4638906 yz=-0.2558797 zz=0.1455125

The F-test implies a significant improvement in the definition of the Pacific Euler vector for the exclusion of each and both stations. This can be explained by the geographic location of GUAZ and CHAT and their resulting relative importance that varies between 26-33% for CHAT and 32-38% for GUAZ. The residual velocities of GUAZ and CHAT with respect to the Pacific plate Euler vectors are close to the limit of the 95% confidence interval error ellipse for 9 of the 11 models. In the model for which GUAZ was excluded we also obtain the largest residual for GUAZ ( $2.6 \pm 0.6$  mm/yr), while CHAT shows a near perfect fit ( $0.4 \pm 0.4$  mm/yr). Stations on the Hawaiian Islands, TUVA, MARC, and TRUK show low residuals. In the model for which CHAT is excluded, the residual of CHAT increases to  $1.9 \pm 0.5$  mm/yr, while GUAZ is better fit ( $0.6 \pm 0.4$  mm/yr), together with good fits at THTI, CKIS, KIRI, and POHN. In general, these results are consistent with a rigid Pacific plate, within limits defined by our data uncertainty,  $\sim 2$ mm/yr.

Our best-fitting Pacific plate Euler vector PA1 is based on 9 stations, excludes GUAZ and CHAT, and has a reduced  $\chi^2$  of 1.00 (Table 1, 2). The station importance for this solution varies between 5 and 21% (Table1). The average residual velocity of the 14 stations on the interior of the Pacific plate is 1.1 mm/yr. GUAZ shows significant residual motion, while CHAT and MAUI have residual velocities close to the error limit (Figure 2.3, Table 1).



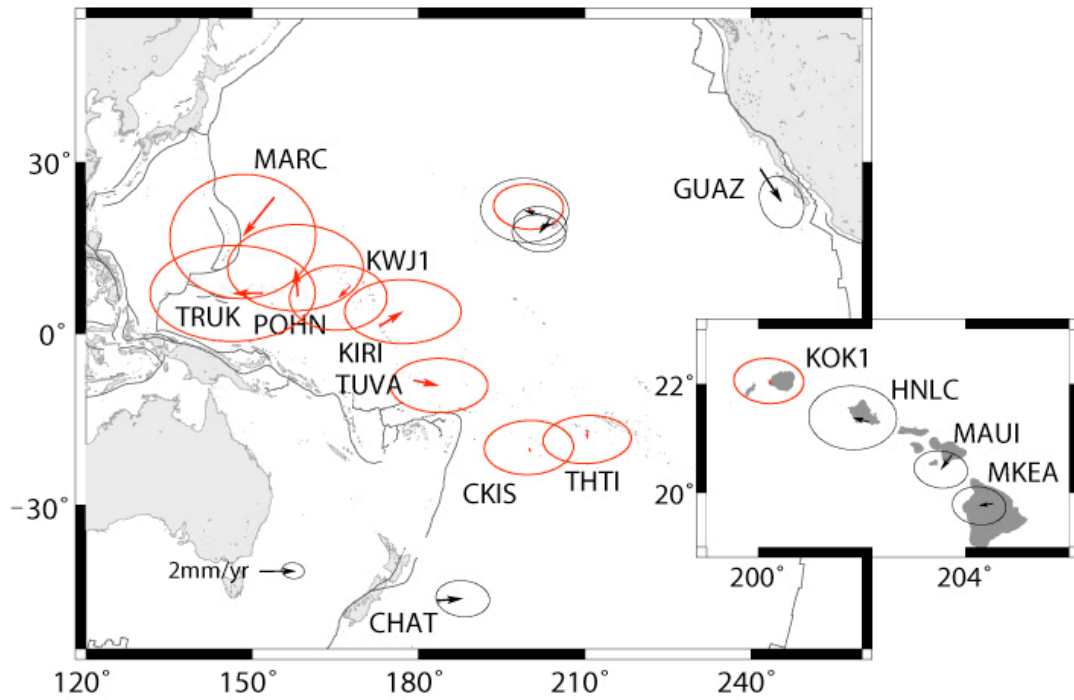


Figure 2.3: Residual velocity with respect to best fitting Pacific plate Euler vector (Table 1). Stations used for the computation of the Euler vector are shown in red. Error ellipses indicate 95% confidence interval, to distinguish significant residual motion. Fault and plate boundaries from the same sources of Figure 2.1.

## Rigidity of the Baja California microplate

Geological observations suggest rigid block behaviour for Baja California (e.g. Gastil et al., 1975; Suarez-Vidal et al., 1991; Umhoefer and Dorsey, 1997; Umhoefer, 2000). The northern and southern ends of the peninsula are cut by several faults, but there is no apparent deformation along the main body of the peninsular batholith. We calculate a Baja California Euler vector using GPS data from stations located within the geologically rigid block (Table 3). The Agua Blanca fault along with the San Pedro Martir fault marks the northern boundary of the block (Figure 2.1). The southern block boundary includes the Bonfil fault, the Carrizal fault and the San Jose Cabo fault (Figure 2.1). We exclude GPS stations LOSA and SPMX, located close to the Agua Blanca fault and San Pedro Martir faults respectively and possibly influenced by strain accumulation (Dixon et al., 2002). The shape of the Baja California peninsula poses problems to an Euler vector calculation due to its limited east-west extent, reflected in the orientation of the ellipsoid describing its uncertainty (Table 2). The best fitting Euler vector has a reduced  $\chi^2$  misfit of 3.5. All residual rates within the geologically rigid block are within uncertainties at 95% confidence (Figure 2.4; Table 3). However, the azimuths of the residuals do not appear to be randomly oriented, as the northern network has its residual motion directed towards the south and vice versa (Figure 2.4). For the northern network the mean residual rate is  $1.7 \pm 0.8$ ; for the south it is  $1.3 \pm 0.8$  mm/yr. This apparent convergence may reflect data uncertainty, or perhaps internal deformation of the block. In the latter case the average shortening strain rate between the two networks is  $\sim 1 \cdot 10^{-16} \text{ sec}^{-1}$ . Additional EGPS data from Baja California will be required to distinguish between these hypotheses.

We tested for the effect of elastic strain accumulation at the edges of the microplate using the block model code DEFNODE (McCaffrey, 2002). We found that stations LOSA and SPMX are affected by strain accumulation when assuming a standard locking depth of the block bounding faults between 10 and 20 km. All other stations within the geologically rigid block are unaffected by strain accumulation. Therefore we believe our Baja California Euler vector adequately represents the rigid microplate motion within the defined uncertainty limits.

We find that sites AGUA, CARD, TOSA and CABO in the southern network move with very similar rate and direction with respect to rigid Baja California. Therefore our geodetic measurements cannot resolve motion across the Carrizal fault, which has sometimes been described to cut through the peninsula (e.g. Hausback, 1984). This suggests that the south-western tip of the peninsula belongs to the rigid microplate (Figure 2.4). Other stations in the southern tip of Baja California may represent the motion of smaller blocks that are bounded by active normal faults. This is compatible with the recent geological observations of Busch et al. (2006).

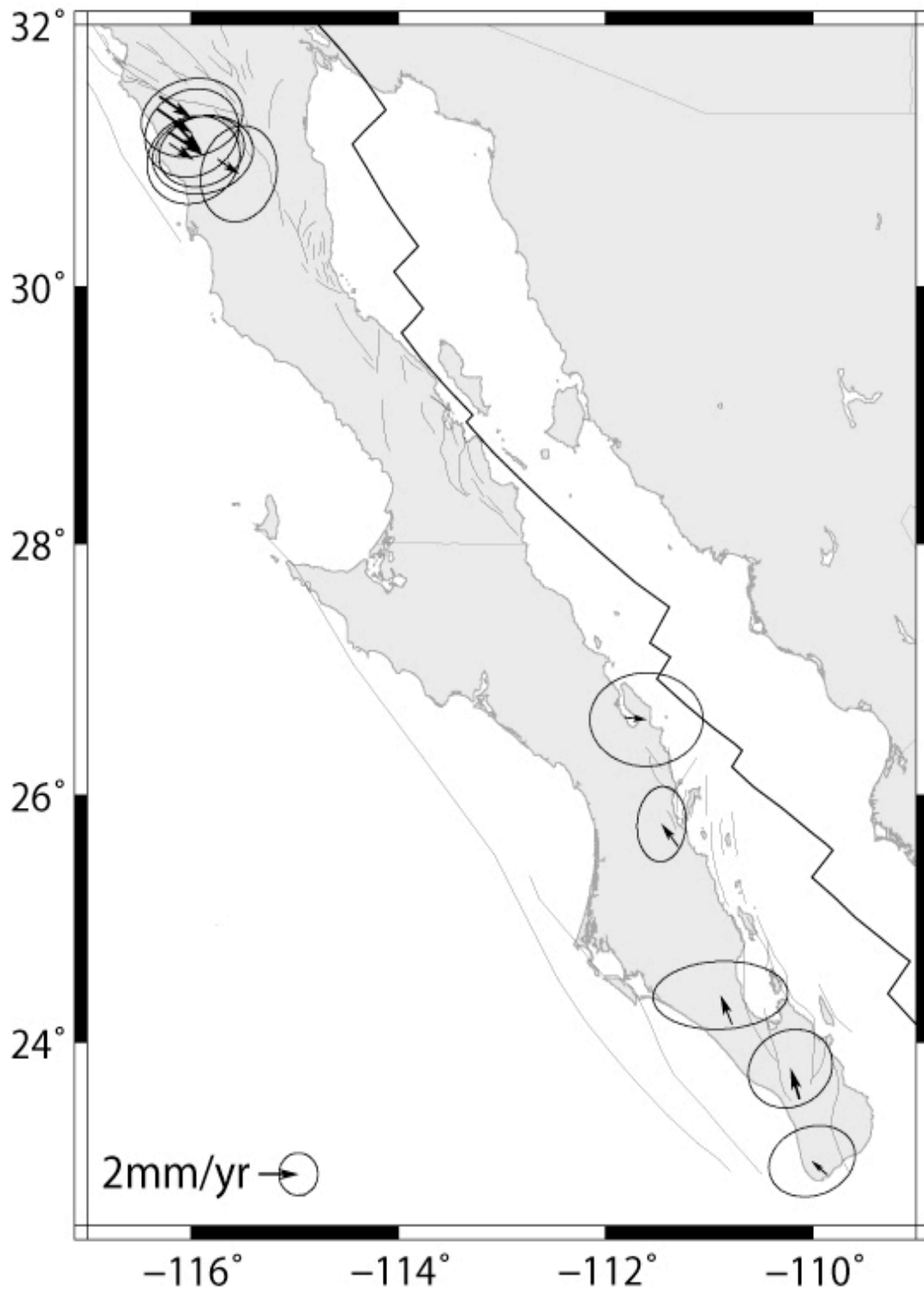


Figure 2.4: Stations on the Baja California microplate: Residual motion with respect to Baja California Euler vector (Table 1). Error ellipses indicate 95% confidence interval.

Table 3: Velocity of GPS stations in Baja California and residual motion with respect to the stable Pacific plate PA1.\*

Site	Lon	Lat.	IGb00				Residual to PA 1			Residual to BAC1		
			Ve	$\sigma$ Ve	Vn	$\sigma$ Vn	Rate	$\sigma$ rate	Azi.	Rate	$\sigma$ rate	Azi.
id	(°E)	(°N)	mm/yr	mm/yr	mm/yr	mm/yr	mm/yr	mm/yr	(°)	mm/yr	mm/yr	(°)
AGUA	-111.30	25.59	-48.4	0.3	19.6	0.6	3.2	0.7	141	1.3	0.6	-39
ancn	-110.03	23.74	-51.0	1.7	18.6	0.7	3.1	1.0	163	2.1	1.7	-75
blnd	-110.31	24.33	-48.7	0.7	20.2	0.7	3.1	0.8	118	2.0	0.8	-5
burr	-110.07	23.52	-48.7	1.3	19.8	0.8	3.8	1.3	117	1.8	0.1	15
CABO	-109.86	22.92	-50.4	0.7	18.6	0.5	3.6	0.7	143	1.0	0.7	-51
CADG	-116.32	31.36	-41.6	0.8	19.5	0.7	6.4	0.9	137	2.0	0.9	123
CARD	-110.78	24.15	-49.3	1.3	19.7	0.5	3.2	1.1	133	1.5	0.8	-23
cice	-116.67	31.87	-40.2	0.9	17.4	0.8	8.8	1.0	142	4.3	0.9	141
COLO	-116.21	31.10	-42.3	0.8	19.8	0.7	5.9	0.9	138	1.4	0.9	122
CONC	-111.81	26.62	-45.7	1.1	18.7	0.8	5.3	1.1	133	1.1	1.2	95
ecer	-109.81	24.18	-48.3	0.9	20.4	1.0	3.3	1.0	108	2.5	1.1	6
elal	-116.21	31.85	-39.8	0.7	20.4	1.0	6.8	0.9	123	3.1	0.9	93
elch	-115.05	31.49	-37.0	0.6	16.2	0.5	11.4	0.7	131	7.1	0.7	123
elco	-116.17	32.47	-37.5	0.7	17.1	0.9	10.2	0.9	134	5.9	0.9	126
elja	-115.76	31.49	-39.9	0.8	18.4	0.6	8.1	0.8	134	3.8	0.9	122
elmo	-116.99	32.27	-39.8	1.1	18.1	1.0	8.4	1.1	139	3.9	1.1	135
emir	-109.74	23.37	-51.3	1.0	17.7	0.6	3.8	0.8	167	2.1	1.1	-89
filo	-116.44	31.72	-40.9	1.5	21.3	1.2	5.6	1.5	122	2.2	1.6	73
inde	-115.94	31.55	-39.4	1.0	18.4	0.6	8.5	1.0	132	4.2	1.0	119
lagh	-115.96	31.97	-37.8	0.9	18.1	0.7	9.6	0.9	128	5.4	1.0	116
losa	-116.3	31.46	-41.6	0.9	19.6	0.6	6.3	0.9	137	1.9	0.9	122
mayo	-115.24	31.99	-35.7	1.7	15.1	0.9	12.8	1.5	133	8.5	1.5	127
MELR*	-115.74	30.98	-42.5	0.6	19.7	0.8	5.7	0.9	139	1.3	0.8	123

rive	-109.53	23.55	-49.5	1.0	20.0	0.5	2.8	1.0	118	2.2	0.7	-11
rlov	-116.63	32.12	-39.2	0.9	18.4	0.8	8.5	1.0	134	4.2	1.0	124
SAIS	-116.22	31.19	-41.7	0.9	19.5	0.6	6.4	0.9	137	2.0	0.9	121
sald	-115.39	31.77	-36.6	1.0	16.5	0.9	11.4	1.1	130	7.2	1.1	121
sfai	-114.81	30.93	-42.8	1.0	16.1	0.7	8.2	0.9	156	4.0	0.8	171
SLRE	-116.16	31.26	-42.4	0.7	19.0	0.5	6.4	0.7	141	1.9	0.7	134
sm01	-115.83	31.62	-41.0	0.9	17.9	1.3	7.7	1.3	143	3.2	1.2	142
spmx	-115.47	31.05	-43.5	0.6	18.3	0.5	6.2	0.7	155	2.0	0.7	-179
TOSA	-110.13	23.54	-49.6	0.7	19.5	0.6	3.2	0.8	130	1.5	0.7	-17
wmar	-111.98	24.51	-50.0	1.4	21.1	1.0	2.0	1.3	131	2.6	1.2	-32

- 
- Column headings are analogous to Table 1.

## **Pacific - Baja California motion**

We tested the significance of a separate Baja California microplate compared to a larger Pacific plate including Baja California by applying the F-test (Stein and Gordon, 1984). Baja California acts as a separate microplate with 99% confidence. Since Guadalupe Island shows significant residual motion with respect to our Pacific Euler vector PA1 we also tested the possibility that it may be part of the Baja California microplate. The F-test indicates that this is not the case at 99% confidence, implying that the western border of the Baja California microplate lies east of Guadalupe Island.

The magnitude of relative motion of Baja California with respect to the Pacific plate depends on the chosen stable Pacific plate reference frame. The relative motion increases when using PA1 + CHAT, while it decreases when using PA1 + GUAZ, with a range of difference of 1.8 mm/yr for the mean relative motion. However all models lead to significant relative motion of the Baja California microplate with respect to the Pacific plate at 95% confidence interval. In the following we use model PA1.

Except for WMAR, all the EGPS velocities in Baja California relative to the stable Pacific plate are significant at 95% confidence interval (Table 3; Figure 2.5a and 2.5b). On the rigid microplate the average velocity with respect to the Pacific plate is 4.9 mm/yr, ranging from  $3.2 \pm 0.7$  (AGUA) to  $6.4 \pm 0.9$  mm/yr (CADG). The average rate of the northern network (CADG, COLO, LOSA; MELR; SAIS, SLRE) is 6.2 mm/yr. In the southern network (AGUA, CABO, CARD, TOSA) the average rate is 3.7 mm/yr. Outside the rigid microplate, deformation of parts of the plate boundary zone can be observed. The

northern part of the peninsula shows an increase of velocity from west to east, approaching the North America - Baja California boundary, i.e., the San Andreas/Gulf of California system. The velocity reaches  $12.8 \pm 1.5$  mm at MAYO, indicating significant strain accumulation along the northern faults (Figure 2.5a). In the southern part of the peninsula no such pattern is observed. West of the peninsula, station WMAR, located on Isla Margarita, shows a velocity with respect to the Pacific plate that is zero within uncertainty (Figure 2.5b).



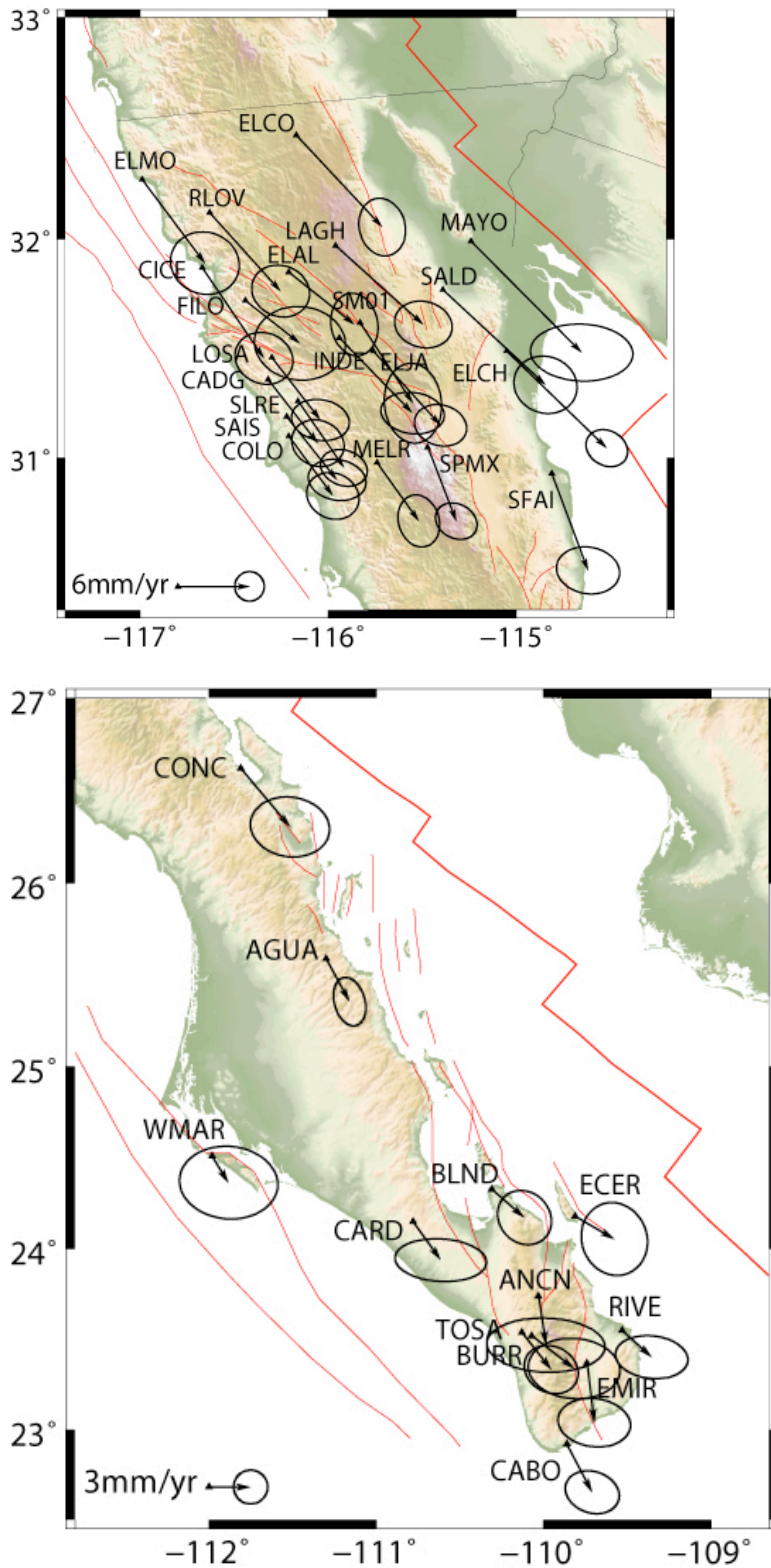


Figure 2.5a and 2.5b: Northern (a) and southern (b) GPS network on Baja California: Velocity with respect to stable Pacific plate Euler vector 1 (Table 1). Error ellipses indicate 95% confidence interval.

## **North America - Pacific motion**

The precision of the geodetic estimates of NA-Pacific motion has improved with time, as more stations become available and GPS time series become longer (Argus and Heflin, 1995; Larson et al., 1997; DeMets and Dixon, 1999; Freymueller et al., 1999; Beavan et al., 2002; Sella et al., 2002; Gonzales-Garcia et al., 2003). Our result for NA-PA1 together with previous results is listed in Table 2, and illustrated in Figure 2.6.

We obtain a shift in the location of the North America - Pacific pole of rotation (Table 2) when we use PA1+CHAT or PA1+GUAZ instead of PA1 for the Pacific plate. The results are comparable to the difference in location of the North America – Pacific pole of rotation from Beavan et al. (2002) compared to the one of Gonzalez-Garcia et al. (2003). This may be because Beavan et al. (2002) use CHAT and EGPS data from the Campbell Plateau (analogous to PA1+CHAT), while Gonzalez-Garcia et al. (2003) use 1 CGPS and 3 EGPS stations from Guadalupe Island (analogous to PA1+GUAZ).

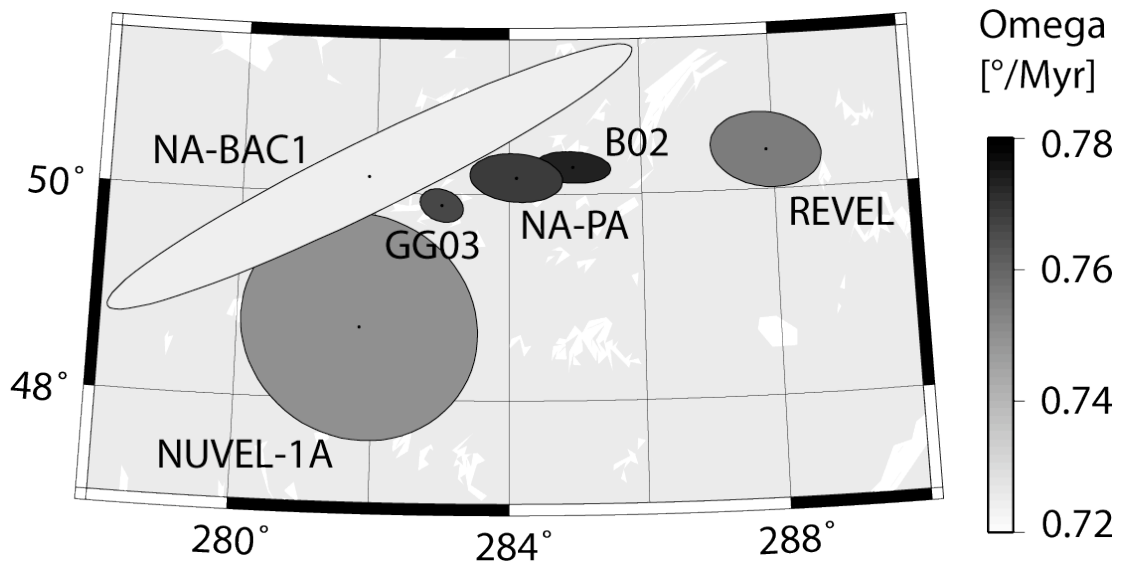


Figure 2.6: Location and magnitude of North America – Pacific (NA-PA) Euler vectors and North America – Baja California (NA-BAC1) Euler vector. If not otherwise indicated, results are from this study. NUVEL-1A (DeMets et al. 1994), Revel (Sella et al. 2002), B02 (Beavan et al. 2002), GG03 (Gonzalez-Garcia et al. 2003). Ellipses show the 1 sigma error from a 2D distribution.

Comparing our Euler vectors we see that the North America – Pacific rotation rate is significantly faster than North America – Baja California. At the location  $23.5^{\circ}$  N,  $108.5^{\circ}$  W, at the spreading centre in the Gulf of California (DeMets 1995), we calculate North America – Pacific motion to be  $51.1 \pm 0.4$  mm/yr at an azimuth of  $125 \pm 1^{\circ}$  clockwise from north. Relative motion between North America and Baja California at the same location is only  $46.8 \pm 0.4$  mm/yr,  $124 \pm 1^{\circ}$  clockwise from north. This leaves a residual motion of  $4.3 \pm 0.8$  mm/yr between Baja California and the Pacific plate. The negligible difference in azimuth, which is also indicated by the proximity of the two Euler poles, shows that Baja California is moving in approximately the same direction as the Pacific plate with respect to North America.

Along the Gulf of California, the geodetic rate for North America - Baja California derived from our Euler vector decreases from south to north,  $46.8 \pm 0.4$  mm/yr ( $23.5^{\circ}$  N,  $108^{\circ}$  W) to  $43.1 \pm 0.4$  mm/yr at the Colorado River delta ( $31.8^{\circ}$ N,  $-114.5^{\circ}$ W).

A key constraint for the North America – Pacific Euler vector in NUVEL-1A (DeMets et al., 1994) is magnetic anomaly data from the Gulf of California. Due to the rigid block motion of Baja California and incomplete coupling with the Pacific plate, this rate must in reality represent North America – Baja California relative motion. When we compare our geodetic rate for North America – Baja California ( $46.8 \pm 0.4$  mm/yr) with the NUVEL-1A rate ( $47.4 \pm 1.2$  mm/yr) at the latitude of the spreading centre ( $23.5^{\circ}$  N,  $108.5^{\circ}$  W) we see that these rates agree within uncertainties. On the other hand, when we compare at the same location our geodetic North America – Pacific rate ( $51.1 \pm 0.4$  mm/yr) with an estimate of DeMets (1995) that excludes the magnetic anomaly data from the Gulf of California and other problematic datasets from

NUVEL-1A, his velocity ( $51.6 \pm 1.9$  mm/yr) agrees with our results (Figure 2.7). This implies that the average spreading rate in the Gulf of California during the past 3 Myr is comparable to the geodetic rate over the last decade and the same is true for the rate of North America – Pacific plate motion. We can exclude thermal contraction of the seafloor to be responsible for the velocity difference between Baja, and also Guadalupe, with respect to the stable Pacific plate as the contraction can explain only ~1.35% of the spreading rate (Kumar et al., 2006), not the observed ~10% of difference.

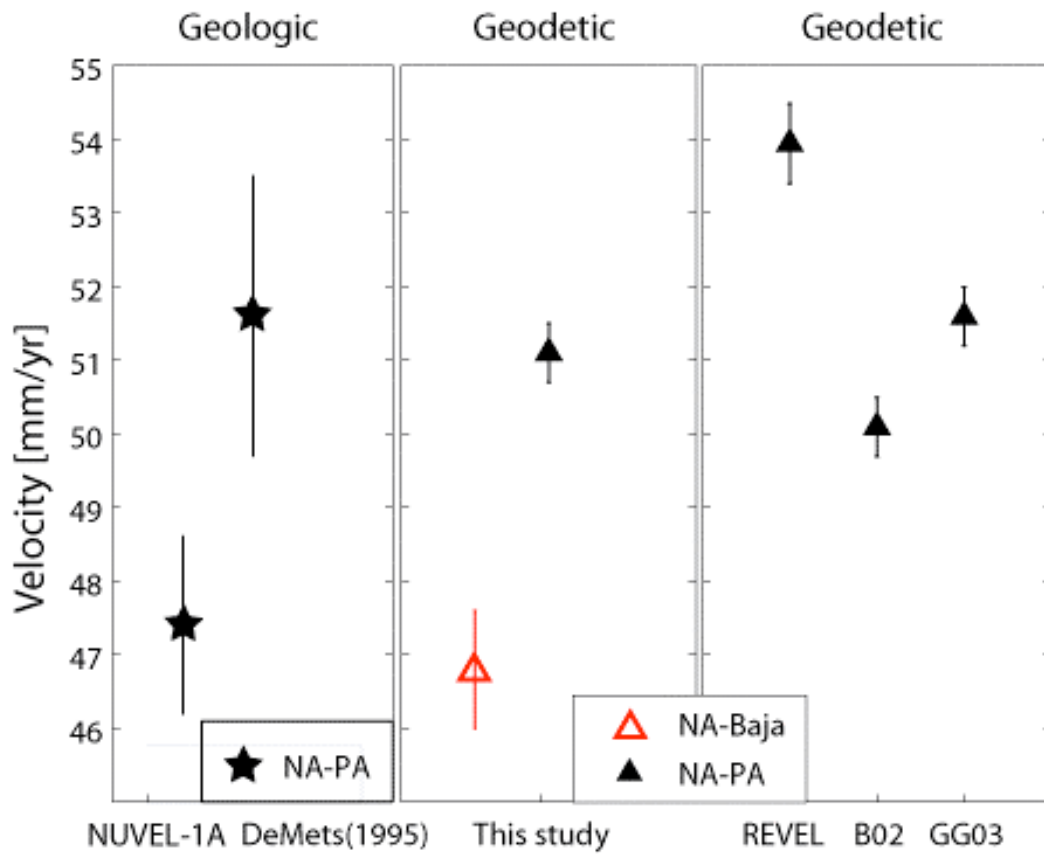


Figure 2.7: Magnitude of NA-PA and NA-Baja relative motion computed for a location at the spreading centre in the Gulf of California ( $23.5^{\circ}$  N,  $108.5^{\circ}$  W). The geodetic rates of NA-PA from different studies (for abbreviations see Figure 2.6) agree with each other and with the rate from geologic model of DeMets (1995). Nuvel1A (DeMets et al., 1994) agrees with NA-Baja.

## Discussion

Baja California and its rigid block motion is an analogue for other terranes that are transported northwest with the Pacific plate while interacting with North America (Atwater and Stock, 1988; McQuarrie and Wernicke, 2005). The essentially rigid behaviour of such a microplate on geodetic time scales preserves the coherence of a terrane during translation over geologic time scales. The correspondence of terrane transport direction with the Pacific plate motion is consistent with the idea that the Pacific plate is the driving force for terrane transport in this region. The subducted extent of the oceanic microplates that were captured by the Pacific plate (Nicholson et al., 1994; Stock and Lee, 1994) may also be an important influence.

The direction of Pacific – North America and Baja California – North America motion is similar, but Baja California moves significantly slower. This result supports the suggestion of a western Baja California shear zone (Dixon et al., 2000b), and is consistent with observations of right-lateral offset on Quaternary faults, and seismicity along the southwestern coast of Baja California (Spencer and Normark, 1979; Legg et al., 1991; Fletcher and Munguia, 2000; Michaud et al., 2004).

A possible explanation for why the Baja California microplate is only partially coupled to the Pacific plate and for activity along the western Baja California shear zone (Dixon et al. 2000b) is the collision of the north-westward moving microplate with North America along the Transverse Ranges and the big bend of the San Andreas fault. This impact may cause the microplate to shear off the Pacific plate, along an inherited weak zone, the former Farallon - North

American plate boundary along the western coast of Baja California. In this case the shear zone may have formed from north to south. This may explain why the northern part of the Baja California microplate shows larger relative motion with respect to Pacific plate than southern part. An alternative explanation for this observed pattern, also consistent with the idea of collision along the northern boundary, is internal deformation within the Baja California microplate.

### **Acknowledgements**

This research is partially supported by DFG. C. Plattner is partially supported by the international graduate school THESIS within the Elitenetzwerk Bayern. R. Malservisi received support from the BMBF, Germany. T.H. Dixon is partially supported by NSF grant OCE0505075. We are very grateful to the operators of the CGPS sites used in this study, including the South Pacific Sea Level and Climate Monitoring Program funded by the Australian Government Aid project operated by Geoscience Australia, the member institutions of IGS, the Western Pacific Integrated Network of GPS (WING) operated by the ERI, and SOPAC. Some of the EGPS data was collected by SCEC, in particular Javier Gonzalez Garcia and Duncan Agnew. We express our gratitude to all people that helped in the collection of the GPS data, in particular the technicians from CICESE. We are very thankful to Paul Umhoefer for providing fault map data, and to Kevin Furlong, Jim Ray, and the reviewers Chuck DeMets and Joann Stock, whose comments helped to improve this paper.



### **3. On the plate boundary forces that drive and resist Baja California<sup>2</sup>**

#### **Abstract**

The driving forces of microplate transport remain one of the major unknowns in plate tectonics. Our hypothesis postulates that the Baja California microplate is transported along the North America – Pacific plate boundary by partial coupling to the Pacific plate and low coupling to the North American plate. To test this idea, we use numerical modeling to examine the interplate coupling on a multiple earthquake-cycle timescale along the Baja California – Pacific plate boundary and compare the modeled velocity field with the observed geodetic motion of the Baja California microplate. We find that when the strain can localize along a weak structure surrounding the microplate (faults), high interplate coupling, produced by frictional tectonic stresses can reproduce the observed kinematics of the Baja California microplate as seen from geodetic rigid plate motions. We also find that the northward motion of Baja California can influence the fault slip partitioning of the major faults in the North America – Pacific plate boundary region north of Baja California.

#### **Introduction**

---

<sup>2</sup> This chapter has been published as: Plattner, C., Malservisi, R., Govers, R., (2009), On the plate boundary forces that drive and resist Baja California, *Geology*, v. 37, p. 359-362, doi:10.1130/G25360A.1

Space geodetic measurements have substantially increased the spatial resolution of the surface velocity field of plate motions over the last decades. Particularly in continental plate boundary regions these data revealed an increasing amount of microplates and rigid blocks. With these subdivisions the meaning of the word “plate” as an individual mechanical entity for which we can apply concepts like torque balance (Forsyth and Uyeda, 1975) becomes less clear. In the classical view, the motion and dynamics of a plate were driven from within by body forces (including ridge push and slab pull), coupling of the plates to the asthenosphere, and frictional sliding along the plate boundaries. However, a common hypothesis is that microplates are externally driven, i.e., that larger neighbor plates determine their motion. The purpose of this paper is to test this “neighbor driven microplate” hypothesis for the Baja California (BAJA) microplate.

Until the early Miocene, the Farallon plate subducted beneath North America (NAM). As the East Pacific Rise approached the trench, subduction of the remnant pieces of the Farallon plate and mid ocean ridge spreading ceased (Lonsdale, 1989, 1991). In the middle Miocene (~12 Ma), extension initiated in a diffuse region along the former volcanic arc (“Protogulf”) east of BAJA (Stock and Hodges, 1989). By the end of the Miocene (~6 Ma) the main plate boundary had localized in the Gulf of California and BAJA was detached from the NAM plate (Lonsdale, 1989).

In Plattner et al. (2007) (see here chapter 2) global positioning system (GPS) measurements were used to show that Baja California (BAJA) is currently moving with respect to NAM in approximately the same direction as the PAC plate, but at a rate that is ~10% slower than the PAC plate. This result agrees with conclusions from geological studies (Fletcher et al., 2007; Michaud et al.,

2004; Nicholson et al., 1994) that BAJA is partially coupled with PAC. The GPS results also imply that BAJA is only loosely coupled to NAM. Here, we address the question how high BAJA-PAC coupling stresses, and how low BAJA-NAM stresses need to be, to reproduce the regional kinematics. The following geodynamic model allows us to independently constrain these plate boundary forces.

### **Model setup**

We solve the mechanical equilibrium equations using the finite element code G-TECTON with (2D) plane stress spherical shell elements (Govers and Meijer, 2001) and a reference thickness of 100 km. East and west model domain boundaries (Figure 3.1) are chosen far from our region of interest. The north-south extent of the model is chosen to encompass the region between the Mendocino and Rivera Triple Junctions. The model is edge-driven by geodetically constrained velocity boundary conditions (chapter 2, table 2) relative to NAM, with two exceptions; 1) the southern boundary of BAJA is left unconstrained to not impose additional driving or resisting forces 2) The northern boundary of the Sierra Nevada (SIERRA) microplate is also free to move, because its interaction with adjacent NAM is undefined. In chapter 2 was demonstrated that the (GPS) instantaneous BAJA-NAM and NAM-PAC velocities are compatible with geologic averages, thus the same edge velocities can be used to drive our mechanical model on both geodetic and geological time scales.

Material properties are homogeneous throughout our model domain for simplicity. On short timescales, the lithosphere between plate boundaries is

approximately elastic. On longer timescales, viscous relaxation occurs in the ductile lower crust and upper mantle while the upper crust behaves in a brittle manner (Kohlstedt et al., 1995), i.e., accumulated stresses are thus relaxed by permanent deformation. Over large areas and long timescales this behavior can be approximately represented by a release of stress during a characteristic period (Lambeck, 1988; Stüwe, 2007). In this paper we represent the lithosphere by a single visco-elastic layer. Young's modulus is 75 GPa, and Poisson ratio of 0.3. We use a reference viscosity  $10^{23}$  Pa s, corresponding with a characteristic (Maxwell) relaxation time of 110 kyr.

In our large-scale model, we ignore local details of the fault-geometry by only including (micro-)plate boundaries along the approximate fault traces (see Model Sensitivity). The NAM-PAC plate boundary follows the San Andreas – Gulf of California fault system, and the model fault west of BAJA the surface trace of the San Benito-Tosco Abreojos fault system (SBTA fault), which is the former trench. The SIERRA-NAM boundary is only well defined south of  $39.5^{\circ}\text{N}$ , along the Eastern California Shear Zone/Walker Lane. North of this latitude the location of this boundary is unclear (Unruh et al., 2003; Wesnousky, 2005). Hence, our model SIERRA/NAM boundary extends only as far north as  $39.5^{\circ}\text{N}$  (see Model Sensitivity). Shear along the San Jacinto and Elsinore faults is simulated by a single fault.

All model faults are vertical (the implication of a vertical PAC-BAJA plate boundary is explained later) strike slip can occur in response to shear stress on model faults (Melosh and Williams, 1989). Seafloor spreading at Gulf of California ridges south of  $27^{\circ}\text{N}$  is modeled by allowing both strike-slip and normal relative motion. Fault intersections are represented by triple overlapping nodes. Most model faults are frictionless, besides the SBTA fault.

We investigate mechanical coupling of PAC with BAJA by varying the dynamic friction along the SBTA fault. This shear stress magnitude is the key parameter of this work.

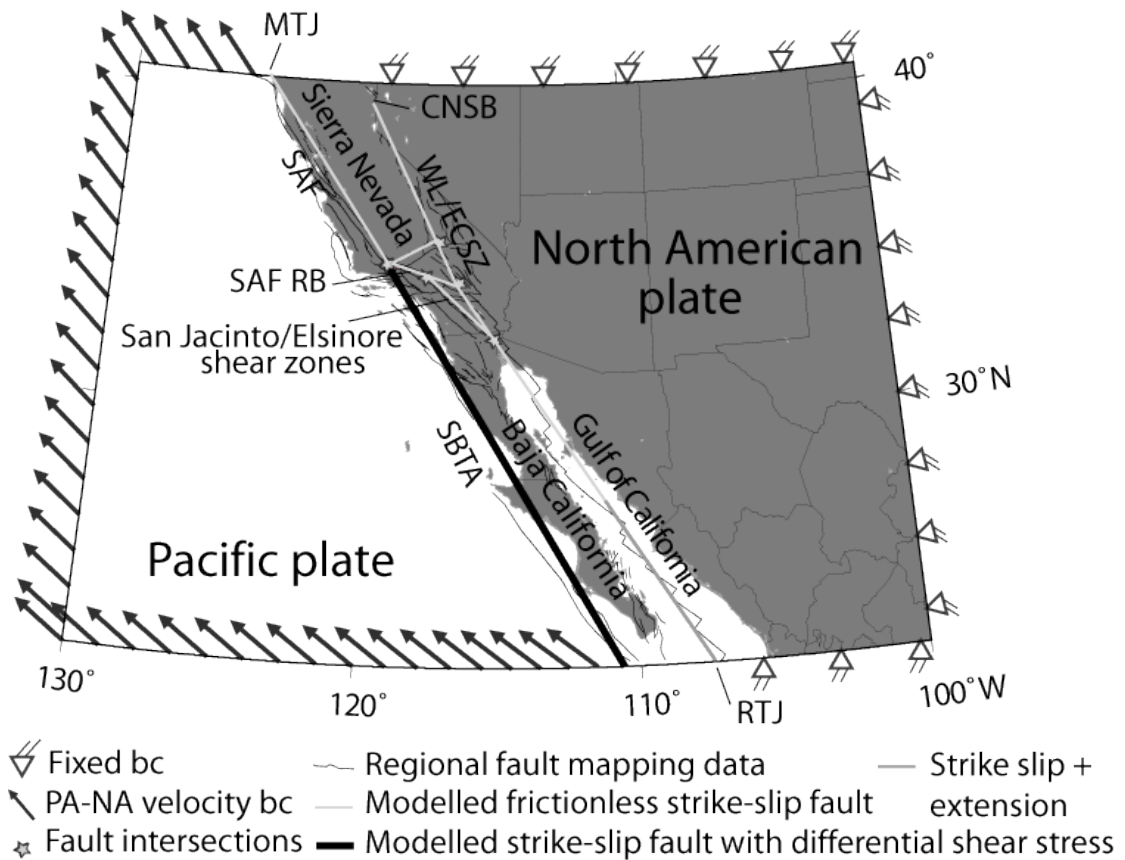


Figure 3.1. Model domain with velocity boundary conditions for fixed North America (velocity vectors here shown in uni-length). The figure shows the major tectonic blocks used in the model. The BAJA micro-plate is coupled with the PAC plate along their common plate common boundary. SAF: San Andreas Fault; SAF RB: San Andreas Fault restraining bend; CNSB: Central Nevada Seismic Belt; WL/ECSZ: Walker Lane/Eastern California Shear Zone; SBTA: San Benito/Tosco Abrejos fault system; MTJ: Mendocino Triple Junction; RTJ: Rivera Triple Junction. Regional faults from (Jennings, 1994) and INEGI (web page <http://galileo.inegi.gob.mx/website/mexico/>; Mexico).

## Modeling results

We first concentrate on the short-term response of the model, for comparison with observations on geodetic timescales (tens of years). This model is essentially elastic. Next, we look at geological timescales (beyond 100 kyr), to examine the consequences of permanent deformation on plate coupling.

### *Plate coupling on geodetic timescales*

To test which fault coupling causes surface displacements that agree with GPS observations we increase the dynamic friction along the SBTA fault from zero (i.e., free slip) until the model BAJA microplate becomes fully locked to the PAC plate. Along a profile at latitude 28°N (Figure 3.2) we look for the frictional shear stress value that optimizes the fit between the model kinematics and the geodetic observations (Figure 3.2). For a frictionless SBTA fault (model not shown here) the partitioning of PAC and NAM plate motion among the faults bounding BAJA is controlled solely by the fault geometry. Approximately half of the total NAM-PAC rate is accommodated on the SBTA fault system and half along the Gulf of California. When we increase the frictional shear stress along the SBTA, fault slip increasingly concentrates on the Gulf of California until the full NAM-PAC relative motion is accommodated east of BAJA (fully locked BAJA).

The model that gives the best fit with the kinematic observations along 28°N is obtained when the friction is 90% of the locking shear stress. For this coupling, the differential motion along the (micro-)plate bounding faults of our numerical model (small dots in Figure 3.2) is in good agreement with the

relative velocities computed from the corresponding Euler poles (chapter 2; Psencik et al., 2006) (large dots in Figure 3.2). A comparison of single model velocity vectors with observed GPS velocities within the rigid BAJA and SIERRA (chapter 2; Psencik et al., 2006) shows agreement within the measurement uncertainty (Figure 3.3).

When the deformation can localize along a weak structure surrounding the microplate (in our case the Gulf of California ridge-fault system) BAJA keeps its geodetic rigidity while being transferred by partial coupling to the PAC plate. However, continuum deformation occurs in regions bounding the model faults (even for a frictionless SBTA fault). This (elastic) strain increases with time (or fault slip) because of the velocity boundary conditions that drive the model. The stresses associated with these strains represent a continuum resistance to microplate motion due to (partial) misalignment of the faults with respect to small circles.

To balance the increasing elastic resistance while keeping the relative plate motions constant, the frictional coupling in the model needs to increase with time. For the best fitting model we need to increase the frictional shear stress along the SBTA fault by 91 Pa/year.

Deformations of the elastic model presented above can only be realistic on a short timescale ( $\sim 1$  earthquake cycle time). On longer timescales it is unlikely that the lithosphere can accumulate infinite stress at the plate boundaries. Therefore, in the next section, we allow for stress relaxation.

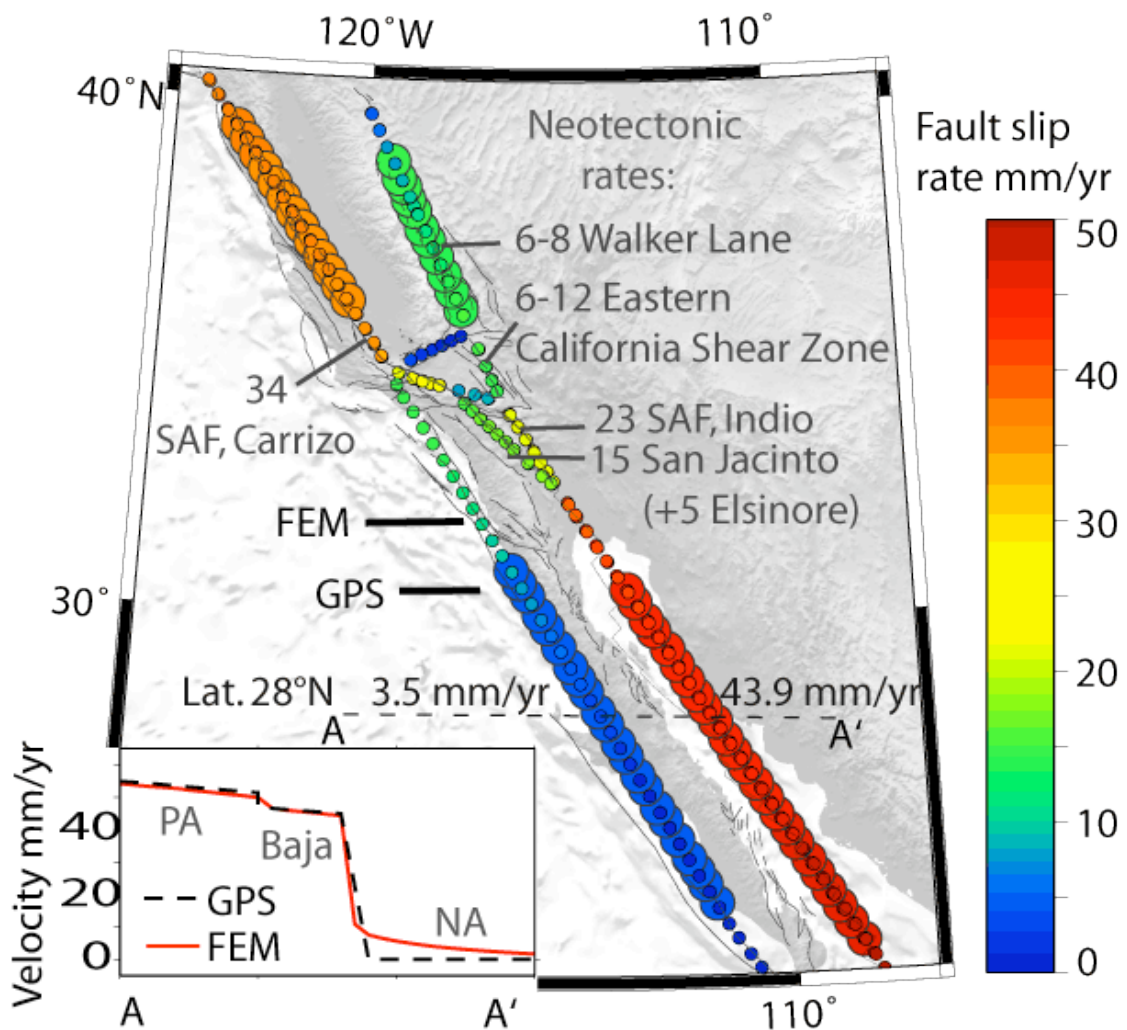


Figure 3.2. Regional fault kinematic for an optimal shear stress applied along the SBTa fault scaled to fit the model velocity (FEM) to the observed geodetic (GPS) rigid plate motion along a profile at latitude 28°N (inset). The model fault velocity (small dots) around the rigid Baja California fits to the corresponding observed geodetic rigid plate relative motions (large dots). The motion of Sierra Nevada microplate induced by the collision of Baja California is also in good agreement with the geodetic rates. Fault slip rates around the San Andreas Fault (SAF) restraining bend agree with neotectonic rates for the corresponding fault system (summarized in Becker et al., 2005).



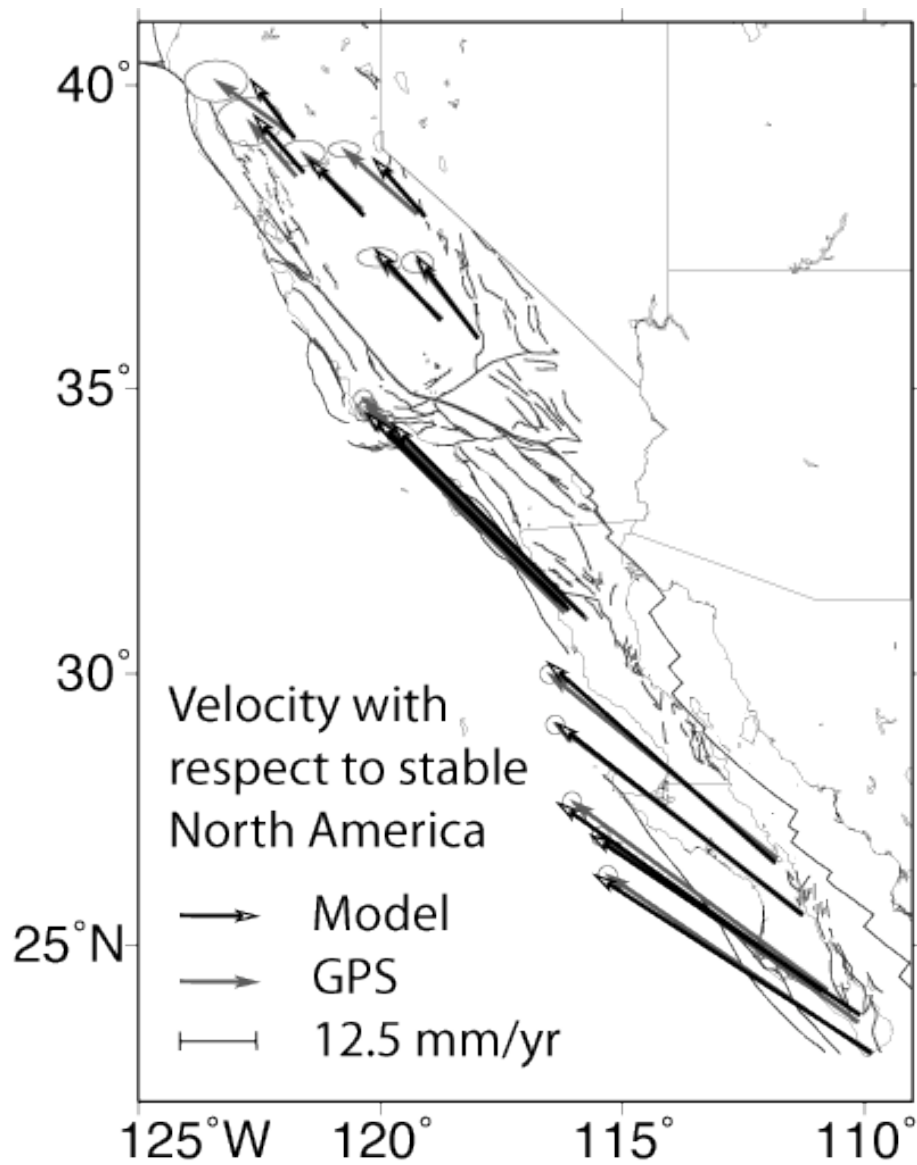


Figure 3.3. Model velocity vectors and GPS velocity vectors from sites located within the rigid BAJA and SIERRA microplates and used for the Euler vector calculations (chapter 2, table 3; Psencik et al., 2006).

### *Plate coupling on geologic timescales*

On timescales that are comparable to, or longer than, the characteristic relaxation time, stress flow (partly) reduces the continuum resistance (Figure 3.4). To maintain the fit with observations, successive coupling stress increments must therefore decrease with time. As a matter of fact, the increment of shear stress decays exponentially at a rate that is controlled by the Maxwell time and by the total applied shear stress along the SBTA. Eventual steady-state represents dynamic equilibrium between the stress increase by loading and decrease by viscous relaxation during a given period. Steady-state is generally reached after a loading period of ~10 Maxwell times. Because of the exponential decay of the applied incremental shear stress the magnitude of the steady-state shear stress along the SBTA fault is equivalent to the initial (elastic) increment multiplied by the Maxwell relaxation time. For the selected Maxwell time of 110 kyr, the steady-state shear stress applied to the SBTA fault is 10 MPa. For a longer Maxwell time, a higher steady-state shear stress is required to activate BAJA motion.

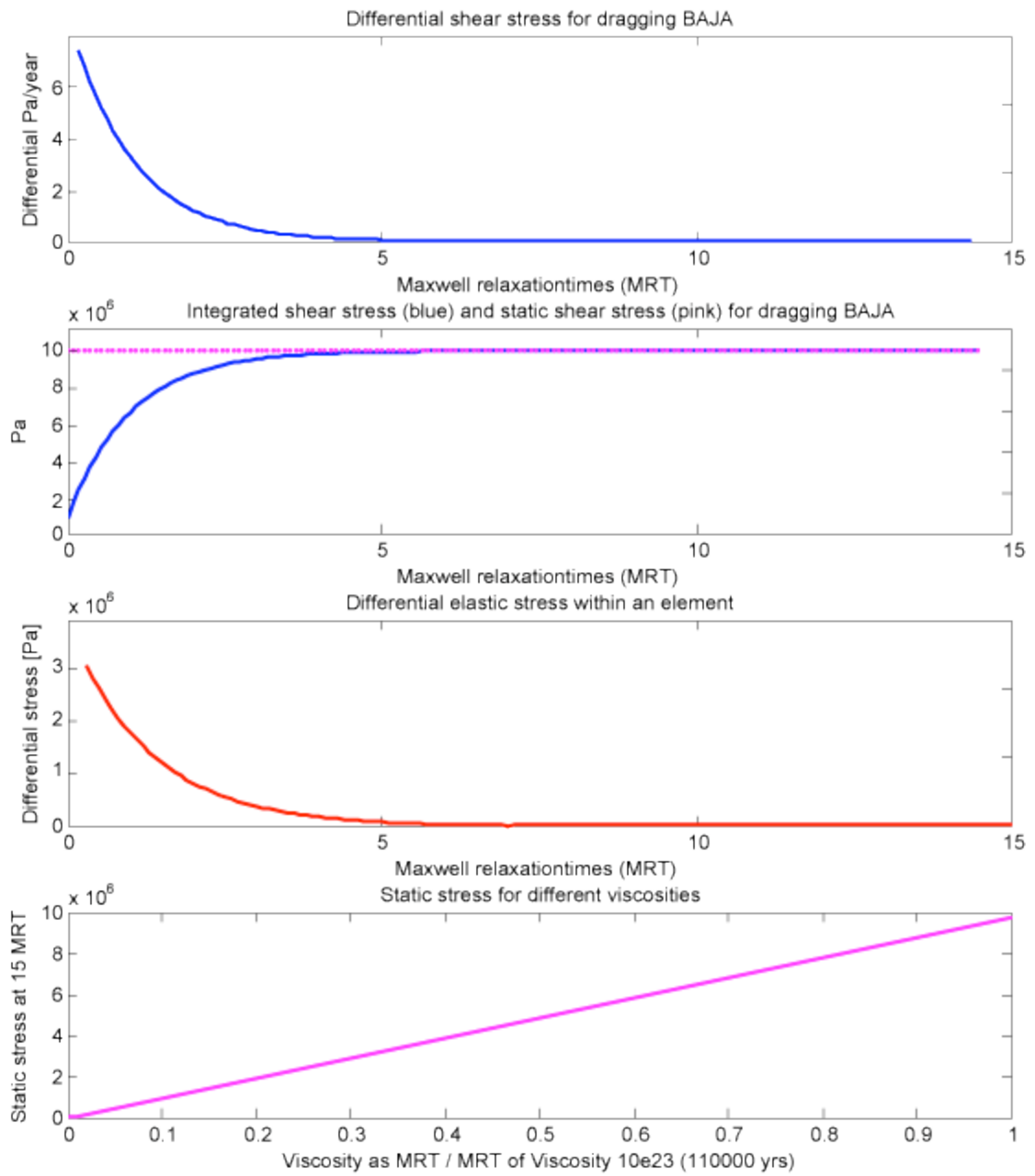


Figure 3.4: Stress relaxation in the viscoelastic model.

## **Model sensitivity**

Where the geometry and location of the most important fault zones in the study area (Figure 3.1) are incompletely known, our choice was motivated by better fit to the GPS observations. Our coupling stress is partly affected by these uncertainties. The coupling stress scales inversely with the length of the SIERRA– NAM plate boundary as the fault length affects the friction between SIERRA and NAM (10% stress variation for length changes within the Central Nevada Seismic Belt). Westward shift of the northern SBTA fault and more northerly connection to the SAF allows BAJA to pass west of the restraining bend shifting motion to the SAF and SIERRA and lowers the coupling stresses (4 MPa for a model in which the northern SBTA continues in the western California borderland and connects along the San Gregorio fault to the SAF). The coupling stress estimate is insensitive to representing the Gulf of California by a sequence of small ridges or basins connected by long transform faults. However, varying the length of the segment that permits an extensional component of slip perpendicular to the Gulf of California boundary can affect the stress by up to 30% (strongly affecting the BAJA velocity azimuth). We did not test how much resisting forces can be lowered by including several smaller fault traces around the restraining bend to simulate continuously deforming areas and the effect of smaller blocks like the Western Transverse Ranges taking up deformation by block rotation. However, we found that not including the San Jacinto or Elsinore fault BAJA rotates clockwise and GPS azimuths cannot be fitted.

In the above models, we assumed that Gulf of California fault is weak. When we increase coupling across this fault, stresses along the SBTA fault need to be increased by the same amount to maintain the fit to the geodetic BAJA

velocities. Coupling stresses in the Gulf of California beyond 5-10 MPa reduce fault slip to the extent that internal deformation starts occurring within BAJA. Detecting such (permanent) internal deformation using GPS is complicated by earthquake cycle signatures from the plate boundaries and the faults located within the GPS network in northern and southern BAJA. As coupling stresses probably decreased over geological time with the progressive localization of strain along Gulf of California ridges and transforms, we would expect that the geodetic strain rate within BAJA of  $10^{-16} \text{ s}^{-1}$  (chapter 2) is lower than average strain rates within BAJA estimated from geology.

The required shear stress to reproduce BAJA motion strongly depends on the length of the coupled segments along the SBTA. Our analysis of geodetic motions only gives the average coupling stress. Reducing this length (while still preserving the velocity field) increases the necessary coupling stress at these segments, and in consequence would introduce local deformation and rotation within BAJA. From geological history it is possible to argue for variations in coupling between fracture zones (Michaud et al., 2006).

## **Analysis**

In our best-fit model, we require a shear stress of 10 MPa on the SBTA fault on geological timescales. This stress magnitude is typical for tectonic stress in the lithosphere (Gardi et al., 2003; Iaffaldano and Bunge, 2008), indicating that BAJA being dragged by the PAC plate is a plausible mechanism. The frictionless fault assumption for all plate boundaries besides PAC – BAJA and the block model geometry yield a lower limit for the lithospheric coupling.

The motion of BAJA induced by coupling with the PAC plate activates faults surrounding the SIERRA microplate. Although SIERRA is not fully decoupled from NAM, the induced fault slip rates along the southern SIERRA plate boundaries are in good agreement with the observed geodetic rigid plate motion of SIERRA with respect to PAC and NAM (dots in Figure 3.2), and with the microplates' velocity field (vectors in Figure 3.3) (Psencik et al., 2006).

The northward motion of BAJA influences the dynamic behavior of the restraining bend fault system (Figure 3.2). Here, a comparison of the model velocity field with GPS observations is not possible since interseismic strain accumulation affects the geodetic data. Regional neotectonic fault slip rates that represent deformation averaged over at least 10 earthquake cycles (Becker et al. 2005) indicate a reasonable fit for the main fault-traces (Figure 3.2).

Our model predicts significant vertical strain along the San Andreas restraining bend, where contraction leads to crustal thickening, and along the Gulf of California, where we predict thinning when fault perpendicular motion is not permitted. The modeled regional pattern of vertical motions is in good agreement with geologic observations. However, rates of crustal thickness change and equivalent uplift or subsidence are significantly smaller than observed. This can be expected since we use a linear rheology that does not allow for localization of the deformation and we do not include effects such as weakening from a pre-existing volcanic arc in the Gulf of California (Fletcher et al., 2007).

## **Discussion and conclusions**

The northward migration of BAJA due to coupling with the PAC plate is hindered in the north by the presence of the SIERRA block and its coupling with NAM. For this reason, development and formation of the eastern boundary of the SIERRA block play a fundamental role in the forces necessary to drive BAJA. An alternative for resisting forces induced by the SIERRA is the presence of a slab window beneath the BAJA microplate lowering the coupling to the PAC plate. However, such a model is only possible with 3D geometry.

A mechanism to increase the coupling along the former plate boundary between NAM and PAC was suggested by (Nicholson et al., 1994). Cessation of spreading between fragments of the former Farallon plate and PAC left slivers of young oceanic lithosphere stalled beneath BAJA. Remnants of these slab fragments beneath BAJA extending all the way out the Gulf of California are interpreted from seismic tomographic images (Zhang et al., 2007). If indeed coupling is due to these stalled microplate fragments, the interface is probably inclined. Because, in our model, we constrained the coupling stress for a vertical interface, the real area of the interface would therefore be larger, and thus would require lower shear stress to generate equivalent frictional forces.

The reproduced kinematics of BAJA and the NAM-PAC plate boundary region, when BAJA is driven by mechanical coupling between BAJA and PAC through tectonically reasonable stresses, suggests that this process is a plausible mechanism for driving the transport of the microplate. Partial coupling and resisting forces to the northward migration of BAJA can be an

explanation for the current motion of the peninsula in the same direction but at a smaller rate of PAC.

## **Acknowledgements**

This research is partially supported by DFG grant MA4163/1-1. CP is partially supported by the international graduate school THESIS within the Elitenetzwerk Bayern. We thank our reviewers for their comments that strongly improved this article. We furthermore want to thank C. Nicholson, J. Fletcher, F. Suarez-Vidal, X. Zhang, P. Umhoefer, for helpful discussions, as well as G. Iaffaldano, O. Heidbach, K.P. Furlong, and H. Pfuhl for helpful comments.



## **4. Development of the Eastern California Shear Zone: Effect of pre-existing weakness in the Basin and Range?<sup>3</sup>**

### **Abstract**

The role that the motion of microplates has played in the development of the Eastern California Shear zone in western North America is unclear. I was previously proposed that shear related to Baja California motion has propagated from the Gulf of California northward into Nevada. However, there is some evidence for earlier formation processes than Baja California motion. Conversely, motion of the Sierra Nevada block may have driven development of an adjacent shear zone. We present a numerical modeling study that examines the deformational response of western North America to Baja California and separately the response to Sierra Nevada microplate motion. In particular we study if, and under what conditions shear strain from these microplate motions can localize in the Eastern California Shear Zone. We find that the Miocene development of lithospheric weakness in the Basin and Range area has a major influence on the shear strain pattern and can facilitate the formation of the northern Eastern California Shear Zone – Walker Lane belt from motion of either or both microplates, moving with respect to North America. If northward motion of the Sierra Nevada microplate occurred

---

<sup>3</sup> This chapter has been submitted to Tectonophysics as: Plattner, C., Malservisi, R., Furlong, K.P., Govers, R., Development of the Eastern California Shear Zone: Effect of pre-existing weakness in the Basin and Range?

prior to Baja California motion, then the development of the Eastern California Shear Zone does not require northward propagation of strain. Increased shear strain and acceleration of fault slip in the Eastern California Shear Zone, in particular in the south adjacent to the Mojave block, would have followed the beginning northward motion of BAJA after 6 Ma.

## **Introduction**

The Eastern California Shear Zone (ECSZ) in western North America is an example of a shear zone within a plate boundary region that is bordered by microplates (Figure 4.1). One proposal is that this shear zone formed by the displacement of the Baja California block in concert with the Pacific plate and the northward propagation of the Gulf of California shear (McCrary et al., 2009; Harry, 2005; Faulds et al., 2005a,b). As the ECSZ marks the eastern border of the Great Valley – Sierra Nevada microplate (SIERRA), this model of shear zone genesis implies, that the SIERRA microplate formed after, and as a result of BAJA motion.

Significant northward motion of BAJA began around 6 Ma following the previous mainly east west oriented Protogulf extension (12 – 6 Ma) (Stock and Hodges, 1989). Geological studies have dated initiation of strike-slip faulting in the ECSZ to 12 – 10 Ma (McQuarrie and Wernicke, 2005; Reheis and Sawyer, 1997), raising the question of whether there was earlier northerly transport of BAJA, or, an additional driver for shear strain in western NAM. Some observations do not support the simple northward propagation of the Gulf of California as an explanation of the formation of the ECSZ. First, there is no obvious connection across the Garlock fault between the northern and

southern part of the shear zones (Dokka and Travis, 1990). Second, as much as 90% of the faulting in the southern part (often also referred to as the Mojave Shear Zone, here called sECSZ) occurred only after 4 Ma (Oskin and Iriondo, 2004; Miller and Yount, 2002). The available observations thus suggest that the sECSZ initiated after the northern ECSZ had already undergone significant shear (to which we refer to as the nECSZ – WLB, including the Walker Lane belt fault zone).

Plattner et al. (2009) showed that with the present-day plate boundary geometry, rigid block motion of SIERRA can be a simple response to BAJA motion. However, the tectonic history of both microplates makes it likely that in the past, and/or even at present, motion of both, the SIERRA and BAJA microplates may have helped drive formation of the ECSZ. Here we test if shear zone formation along the ECSZ could initiate from motion of SIERRA driven by its coupling along the PAC plate boundary, similar to driving forces suggested for BAJA (Nicholson et al., 1994; Plattner et al., 2009). To investigate the deformational response of western NAM to SIERRA block motion and compare these results with the response of western NAM to BAJA motion, we numerically model the result of such microplate motions. We want to address i) if, and under what conditions SIERRA motion can lead to high shear zone formation at the nECSZ - WLB and ii) if, and under what conditions shear zone formation in the nECSZ – WLB from BAJA motion is possible prior to the formation of the sECSZ, and iii) how the formation of the sECSZ may have been influenced by an earlier formation of the nECSZ. In our analysis we are also testing the conditions under which shear zone formation is enhanced by pre-existing weaknesses in the Basin and Range adjacent to the SIERRA block.

## **Model description**

To address these questions, we test two end-member models of the role that the motion of the BAJA and/or SIERRA microplates could play in driving the development of a shear boundary in either of the two ECSZ domains. In each of these models one of the microplates is driven by velocity boundary conditions while the other microplate and NAM passively respond. For both model sets we test the deformational response in western NAM, in particular we assess whether a shear zone could form along the nECSZ – WLB, and within the sECSZ in response to the specified microplate motion. Additionally, we vary the regional rheology of the model to evaluate the possible role played by the previous thermal-deformational history of the Basin and Range in favoring shear zone development between the SIERRA and the Basin and Range. Finally for a subset of models, we test if reactivation of normal faults in the Basin and Range is a necessary condition for development of a localized nECSZ - WLB.

For this numerical modeling we use the finite element code G-TECTON with (2D) plane stress spherical shell elements (Govers and Meijer, 2001) to solve the mechanical equilibrium equations and produce the deformation pattern associated with the different boundary conditions and/or model geometries. The model domain is similar to Plattner et al. (2009) not including the PAC plate but representing it by boundary conditions (Figure 4.1). Since the patterns of strain accumulation in the sECSZ and the nECSZ – WLB are the key outcomes of our models, these fault traces are not included in most of the models, as are faults younger than from late Miocene (Protogulf weakness is simulated by a passive fault, but the presence of this fault does not influence our results significantly).

The NAM plate is fixed with the exception of its northern boundary, which is free to allow northward motion. Free slip boundary conditions in the north give lower resisting forces for BAJA and SIERRA motion, while fixed model boundaries provide an upper limit (the influence of our choice on the model results is discussed in chapter model sensitivity). For each of the end-member models (BAJA or SIERRA driven) we simulate the motion of the block by applying velocity boundary conditions (plate motion with respect to a stable NAM) along the western model boundary (Figure 4.1) to simulate the kinematics from partial lithospheric coupling with the PAC plate along the plate boundary. The BAJA – NAM motion (rotation) is derived from Plattner et al. (2007), while SIERRA – NAM motion (rotation) is derived from Psencik et al (2006). The model rheology is viscoelastic, with the average viscosity of  $10^{23}$  Pa. s for a nominal lithosphere thickness of 100 km. In the first sets of models the viscosity is homogenous over the entire model domain. We also test the effect of weakening in the Basin and Range due to middle Miocene extension (Figure 4.1) to investigate the role that such a rheological contrast can play in the strain pattern in western NAM. Thus, viscosity in the Basin and Range is set to a lower regional average value of  $10^{21}$  Pa. s (Flesch et al., 2000). We have further analyzed the role that pre-existing normal faults in the Basin and Range could play by running a subset of models with homogenous rheology but adding a discrete, free-to-slip fault along the western Basin and Range border (Figure 4.1).

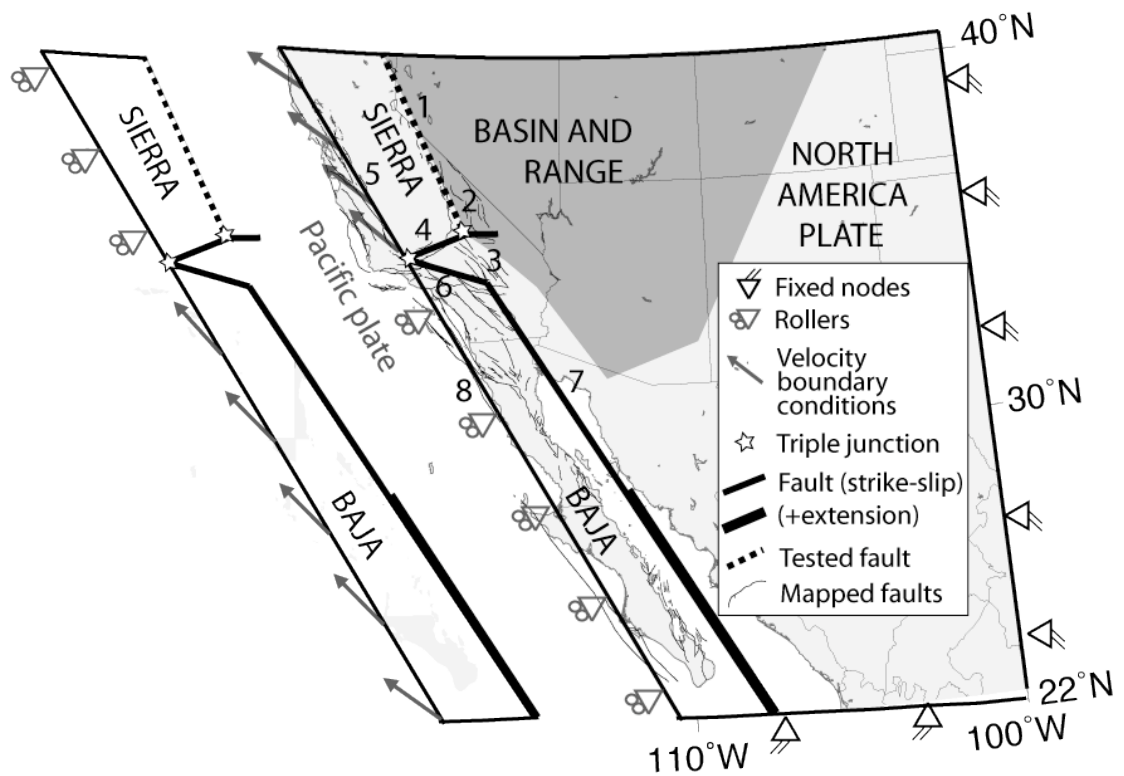


Figure 4.1: Right side shows full model geometry and boundary conditions for the Sierra Nevada (SIERRA) driven model, left side shows only the alterations to model geometry for the Baja California driven model. Model domain boundaries and model faults represent: (1) Walker Lane belt, (2) northern Eastern California Shear Zone, (4) Garlock fault, (5) San Andreas Fault (SAF), (6) SAF restraining bend, (7) BAJA – NAM plate boundary (Gulf of California), (8) PAC – BAJA plate boundary. Geographical region of the southern Eastern California Shear Zone is located at (3), the Mojave block between (3), (4), and (6). The tested weaknesses in NAM are i) the Basin and Range area as a rheological weak zone (dark shaded region), ii) strike-lip fault along dashed line corresponding to (1) and (2).

## **Model results**

To compare the response of NAM to BAJA or SIERRA motion, we investigate the patterns of shear strain generated by the two end-member models. For each of these two models (i.e. BAJA driven or SIERRA driven) we also test the effect of pre-existing weakness in western NAM to evaluate under which conditions shear zones form at the nECSZ – WLB and the sECSZ. Model results parameterized as shear strain rates are shown in both map view and along two profiles oriented perpendicular to the plate motion. The northern profile crosses the nECSZ – WLB approximately at the location of the 1872 Owens Valley earthquake (Hough and Hutton, 2008), the southern profile crosses the sECSZ approximately at the location of the 1999 Hector Mine earthquake (Sandwell et al, 2000) (Figure 4.2). The shear strain rate is calculated as the derivative along the profile using the plate motion parallel velocity. We assume that shear zones most likely form in regions where the shear strain rate is high and the strain localized along a narrow zone.

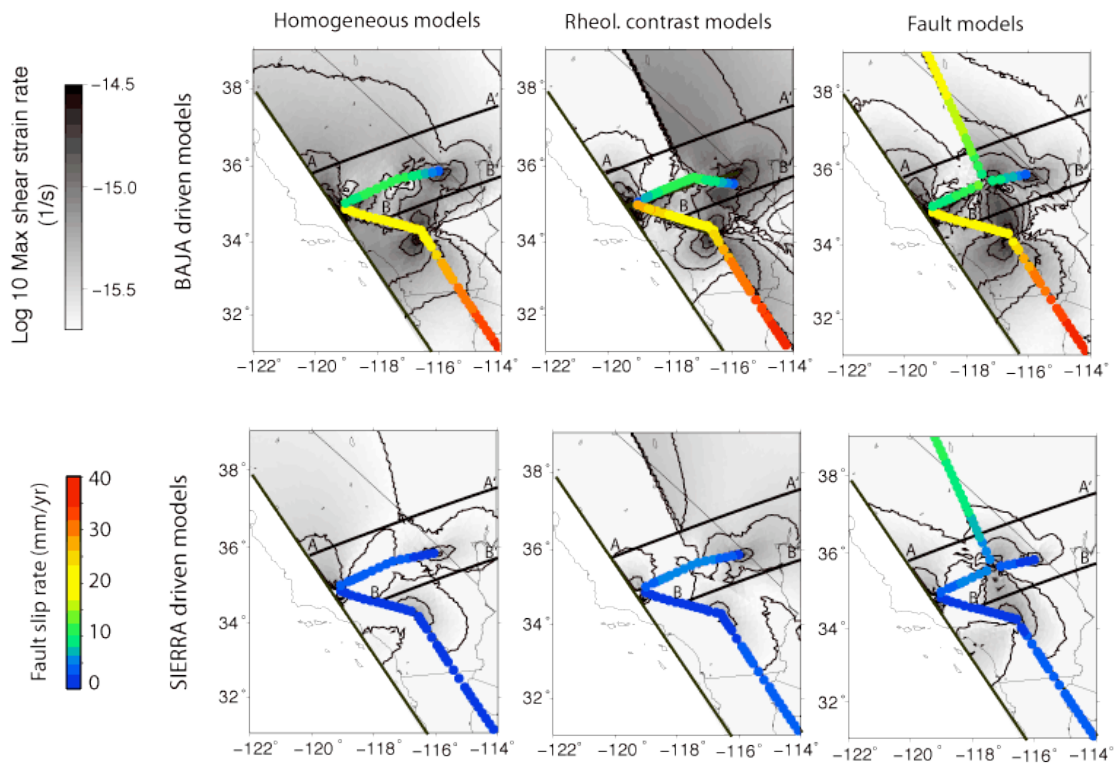


Figure 4.2: Pattern of maximum shear strain rate (logarithmic color scale) in southwestern North America (NAM) as a response to BAJA motion (upper images) respectively SIERRA motion (lower images) and in dependency of the strength in western NAM (see column headers). Maximum shear strain derived from constant strain element information (does not show strain localized by fault slip on between elements). Faults are shown color-coded by the slip rate (not including triple junctions). Profiles A-A' at nECSZ and B-B' are used for strain analysis (Figure 4.3).



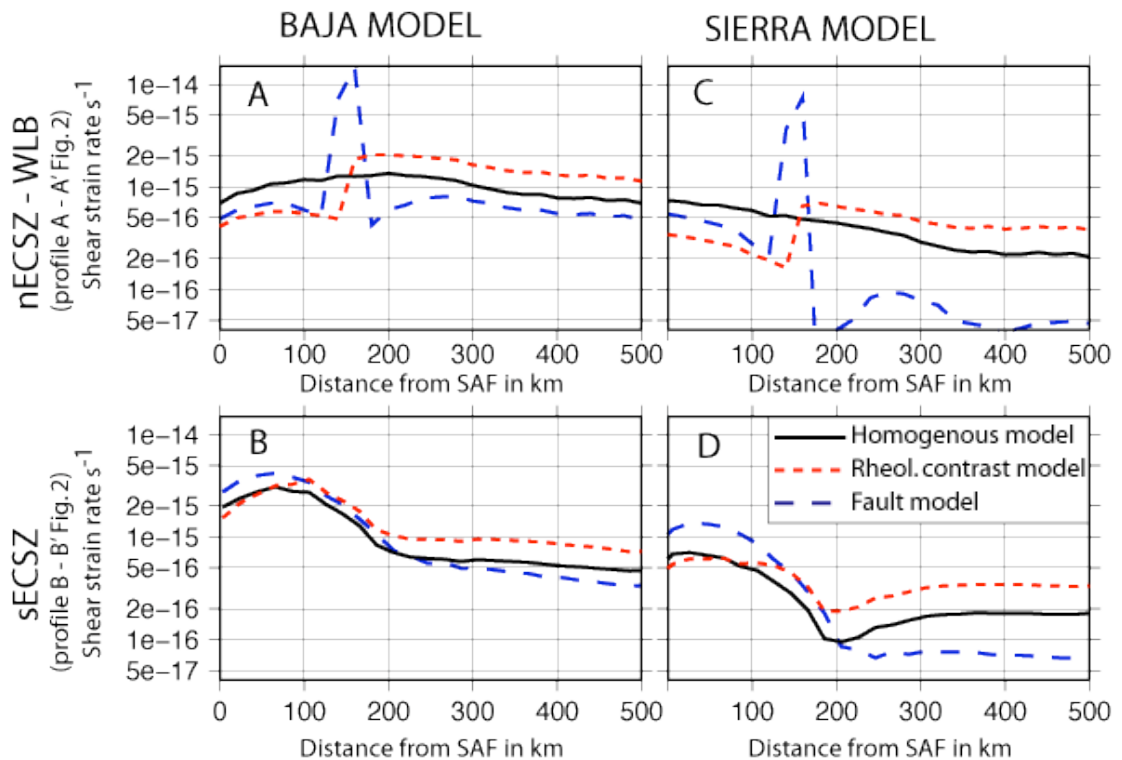


Figure 4.3: Shear strain rate with respect distance from San Andreas Fault (SAF) along the cross-sections A-A' crossing the northern Eastern California Shear Zone – Walker Lane belt (nECSZ - WLB) and B-B' crossing the southern Eastern California Shear Zone (sECSZ) (for location of profiles see Figure 4.2). Left side shows results from models driven by Baja California (BAJA) motion (A, B), right side by Sierra Nevada (SIERRA) motion (C, D). BAJA motion causes larger shear strain in the region of the sECSZ. From both microplate motions shear zones along the nECSZ – WLB can form in case of pre-existing weakness in western North America, such as lower viscosity in the Basin and Range area (rheol. contrast model) or fault zones in the Basin and Range (fault model). Without such weakness (homogenous model) the deformation is broadly distributed over western NAM.

### *Response to Baja California microplate motion*

The motion of BAJA is driven by a velocity boundary condition of approximately 47 mm/yr with respect to fixed NAM along its western border (Figure 4.1). While most of the microplate moves as a rigid block with fault slip along the Gulf of California, its northwestward motion is hindered by the SAF restraining bend, causing deformation in and around this collision zone. The amount and pattern of shear strain from this collision depends on the presence or absence of weakness in western NAM. However, a constant results for all BAJA driven models is that shear strain is localized at the restraining bend corners and at the eastern end of the Garlock fault (Figure 4.2).

#### *a) Homogenous NAM*

The strongest heterogeneity in shear strain is caused by the SAF restraining bend corners and the eastern end of the Garlock fault (Figure 4.2). North of the Garlock fault along the profile A-A' (i.e. nECSZ – WLB, Figure 4.2), shear strain rates are almost constant indicating no localization (Figure 4.3 A). South of the Garlock fault, along the profile B-B' (i.e. sECSZ, Figure 4.2) there are high shear strain rates up to a distance of 200 km from the SAF restraining bend (Figure 4.3 B), with a local maxima at about 80 km corresponding to the present-day location of the sECSZ. The deformation shows a preferred shear orientation to the northeast (Figure 4.2).

#### *b) Pre-existing weakness in western NAM*

If there is a lower viscosity in the Basin and Range, this implies that a higher amount of total shear strain is accommodated in that region. Shear strain rates are also high in areas between the Gulf of California and the western

Basin and Range (Figure 4.2). Low shear strain rates are found in BAJA and SIERRA indicating rigid block motions (Figure 4.2). Along the northern profile, the rheological contrast at 150 km distance from the SAF produces a sharp increase in the shear strain rate curve from low rates at SIERRA to high rates in the Basin and Range (Figure 4.3 A). In the Basin and Range itself, the shear strain localizes near the rheological contact and decays to the east (Figure 4.3 A). Along the southern profile shear strain localizes again in the sECSZ but with higher rates and slower decay east of it (Figure 4.3 B).

We also tested the effect of mechanical discontinuities (pre-existing fault zones) on the deformation pattern. Our model-fault along the nECSZ – WLB (Figure 4.1), which is allowed to slip in its strike direction, is activated as a right-lateral strike-slip fault with slip rates up to 25 mm/yr in the north (Figure 4.2). The accommodation of shear strain on the fault reduces the shear strain in the Basin and Range with respect to the rheology contrast model (Figure 4.2). In SIERRA, shear strain rates are only slightly higher than in the rheological contrast model indicating that also in this case SIERRA is moving as a quasi-rigid block (Figure 4.2). In the strain profile, the strain at the fault appears as a local peak at distance 150 km from the SAF, with low strain rates in the SIERRA and the Basin and Range (Figure 4.3 A).

#### *Response to Sierra Nevada microplate motion*

The velocity boundary conditions applied at the eastern SIERRA border initiate about 14 mm/yr transtensional motion with respect to NAM (Figure 4.1). This motion affects mainly the regions adjacent to the SAF, like the SIERRA and Basin and Range, where the deformational response in western NAM depends strongly on the presence of pre-existing weakness. Strain rates

in the south, in BAJA and around the SAF restraining bend are lower.

*a) Homogenous NAM*

North of the Garlock fault along the profile A-A' (Figure 4.2) shear strain rates are highest east of the SAF and gradually decrease with distance from the SAF without any apparent strain concentration at the nECSZ - WLB (Figure 4.3 D). South of the Garlock fault, there is broadly distributed shear strain around the eastern San Andreas Fault restraining bend corner and the eastern end of the Garlock fault. There is no preferred orientation of the shear strain pattern observable in the region of the sECSZ (Figure 4.2)

*b) Pre-existing weakness in western NAM*

As for the BAJA driven case, lower viscosity in the Basin and Range implies a higher shear strain accommodation there. The SIERRA and BAJA have low strain rates indicating rigid block motions (Figure 4.2). Along the northern profile the rheological contrast at 150 km distance from SAF is evident by the sharp increase in the shear strain rate from low rates at SIERRA to high rates in the Basin and Range (Figure 4.3 C). Within the Basin and Range there is high shear strain near the rheological contact with strain rates decaying exponentially to the east (Figure 4.3 C). South of the Garlock fault along the profile B-B' a broad area of shear strain is found in the area around the SAF restraining bend corner and in the Basin and Range, with lower rates in between (Figure 4.3 D).

When a discrete fault is introduced, up to 12 mm/yr of differential motion between SIERRA and the Basin and Range is localized on the fault (shear strain rate peaks at the fault at a distance of 150 km from SAF, Figure 4.3 C). While some shear strain remains within the SIERRA, the Basin and Range

has shear strain rates close to zero (Figure 4.3 C). South of the Garlock fault shear strain localizes along the sECSZ (Figure 4.3 D), with the map view showing a preferred orientation of the shear zone towards the nECSZ - WLB (Figure 4.2).

### **Model sensitivity**

Details in the shear strain rate pattern in western NAM vary as a result of how a pre-existing weakness in the Basin and Range is represented in our model. The strain pattern is influenced by the geometrical properties of the weak zone, in particular its regional extent and the vicinity of the western Basin and Range border to the stress-source. Similar, the effectiveness of the fault to accommodate stresses depends on its distance and orientation to the stress-source/ stress-field. Multiple, parallel faults broaden the shear strain pattern in the nECSZ – WLB when slip is partitioned among them. For SIERRA motion the stress-source is shear along the western model boundary, for BAJA motion the stress-field is a result of the eastern corner of the SAF restraining bend.

As mentioned before, the northern model boundary condition is not very well defined. This boundary does define the interaction of the model domain with the surrounding plates limiting the northward motion of the studied region. Also in this cases we checked the effects of to end member boundary condition: a completely free north and a completely fix north. In reality the expected behavior would be between these two cases. A free northern boundary associated with velocity boundary conditions applied at the western and eastern border is equivalent to the application of a simple shear to the

entire model domain, mainly adding a constant to the analyzed shear strain rate (or a constant slope in the velocity field). This results in a higher than expected final velocity of the full western North America (Figure 4.4). Interestingly enough, the higher rate of the Sierra Nevada block is compensated by a higher northward migration of the Basin and Range province in a way that the relative strain partitioning does not change significantly. Fixing the northern boundary of the model is equivalent to a reduction of the simple shear applied to the model with a significant reduction of both the velocity of Basin and Range and Sierra Nevada block. The contemporary reduction of the velocity of both blocks does not change significantly (a part for the subtraction of a constant shear strain) the partitioning of strain in the study region (as indicated by the shape of the two strain curves along the two profiles in Figure 4.4). The similarity of the two strain rate profiles for the two end member boundary conditions indicates that the effects of pre-existing mechanical weakness within the model play a fundamental role in the strain partitioning between the different regions independently by the far field boundary conditions. It also suggests that the study region is also sufficiently far away from the effects of the interaction from the northern boundary.

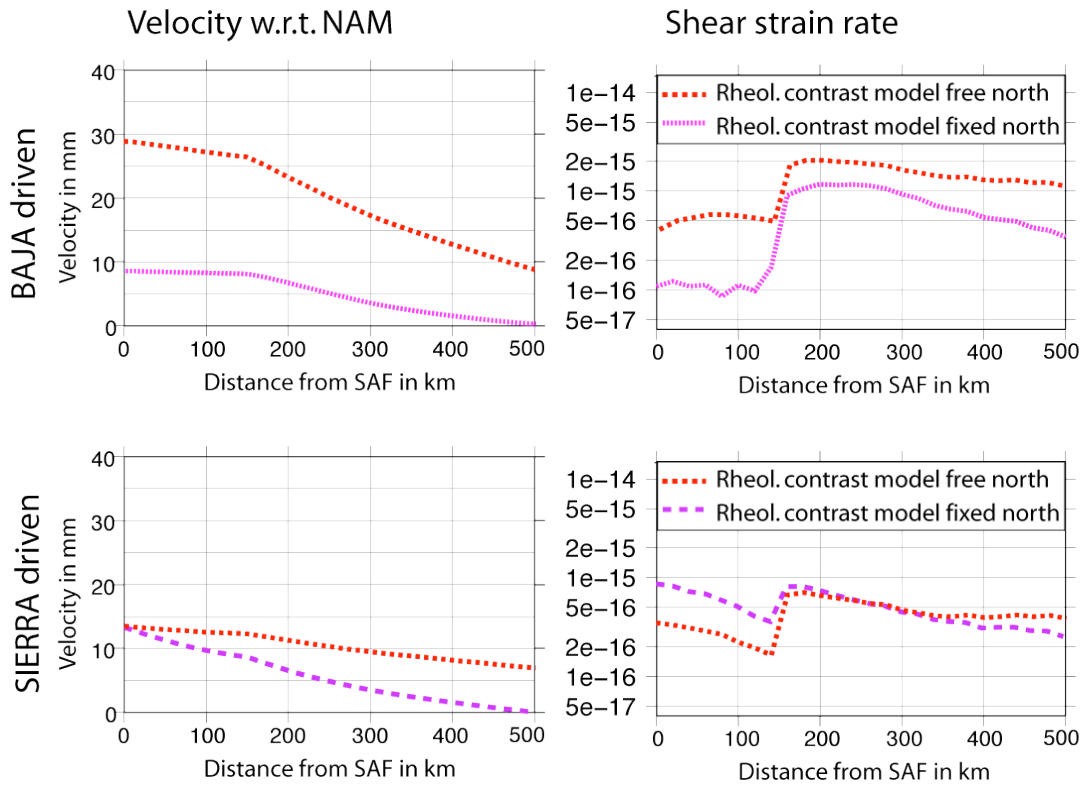


Figure 4.4: Influence of northern boundary conditions on the velocity and shear strain rate across the northern Eastern California Shear Zone – Walker Lane belt (profile A-A' in Figure 4.2), for BAJA driven (upper), and SIERRA driven (lower) models with rheological contrast. Fixing SIERRA and North America in the north decreases the motion of SIERRA in the BAJA driven models. This velocity decrease leads to lower shear strain rates. For the SIERRA driven model the velocity decreases only away from the applied velocity boundary conditions at the San Andreas Fault (SAF), causing higher shear strain rates within SIERRA. However, in all models shear strain still localizes at the rheological contrast, within the Basin and Range.

## Analysis

The results from our models show that pre-existing lithospheric weakness in the Basin and Range can play an important role on the regional strain pattern. In particular lower viscosity and/or pre-existing normal faults within NAM lead to concentration of shear strain that can produce a shear zone formation in the nECSZ – WLB independently of the driving microplate.

In all BAJA driven models shear strain localized at the sECSZ, in agreement with results from Li and Liu (2006) that the geometrical complexity of the SAF is a key component of this shear zone formation. These results suggest, that there is no need for a pre-existing local weakness at the sECSZ, or an intrinsically stronger Mojave block in order to localize strain and initiate the sECSZ. Without any strength heterogeneities in western NAM (weak Basin and Range or pre-existing normal faults) the nECSZ – WLB would form primarily by northward propagation of the sECSZ. However, the presence of strength heterogeneities allows the localization of farfield stresses from BAJA – western NAM collision prior to the formation of the sECSZ. In this case, strike-slip motion at the nECSZ – WLB would have started with the beginning northward motion of BAJA with respect to NAM (approximately 6 Ma). As a result, such a pre-existing weakness leading to shear strain concentration in the nECSZ – WLB influences the shear strain pattern in the sECSZ, both in the total strain rate and the strain pattern.

If SIERRA motion is the driver for ECSZ development, the location of the nECSZ – WLB can best be explained by a strength heterogeneity between the Basin and Range and the SIERRA block, such as lower viscosity and/or pre-existing faults from earlier Basin and Range normal faulting. Shear strain



could have localized in the nECSZ earlier by coupling along the SAF (PAC – SIERRA/NAM plate boundary), e.g. by driving forces similar to lithospheric coupling of microplates along the SAF (Nicholson et al., 1994). In this case, northward propagation from the Gulf of California plate boundary is not needed to produce a shear zone north of the Garlock fault. Once the shear strain is localized along the nECSZ – WLB, this strain accommodation from SIERRA motion can also influence the strain pattern at the sECSZ - even a southward propagation of shear strain would have been possible!

## **Conclusions**

Initiation of strike-slip faulting in the nECSZ – WLB has been dated to 12 – 10 Ma (McQuarrie and Wernicke, 2005), and BAJA motion began only after 6 Ma. We argue that these seemingly inconsistent observations can be explained if SIERRA motion was/has been a driver for early shear strain at the nECSz – WLB, with the strain concentration being caused by pre-existing weakness in the Basin and Range. After 6 Ma, BAJA motion became an important driving force for shear strain in western NAM, accelerating strike-slip faulting in the nECSZ – WLB and driving shear zone formation at the sECSZ.

## 5. CONCLUSIONS

The analysis of horizontal velocity data derived from GPS proved that Baja California (BAJA) is a microplate rather than just a part of the Pacific (PAC) plate (Plattner et al., 2007; see here chapter 2). Its relative motion to the PAC plate involves activity of strike-slip faults offshore BAJA to the west. Across the North America (NAM) – PAC plate boundary region, 10% of the plate relative motion is accommodated between PAC – BAJA, and 90% between BAJA – NAM (in the Gulf of California). An implication of this finding is, that the widely used geologic plate motion model NUVEL-1A (DeMets, 1994), which estimates the full PAC – NAM rate from the Gulf of California mid ocean ridge spreading, gives a 10% underestimated velocity. This geologic 3 Myrs average rate agrees with the present-day geodetic BAJA – NAM rate, suggesting constant plate relative motion since 3 Ma. Constant plate motion for the last 3 Myrs was also found for PAC – NAM (using a geologic plate motion model that excludes the Gulf of California, DeMets, 1995). This agreement justifies using the geodetic rigid plate rotations for numerical simulations with model runtimes of a few Myrs (geological time-scale) to learn about the microplate and plate boundary dynamics.

The similarity of plate motion rate and azimuth suggests partial coupling of BAJA and the PAC plate. Using this coupling as a mechanical driving force for BAJA, the numerical simulation presented in chapter 3 (Plattner et al., 2009) successfully reproduced the geodetic rigid plate motion. Results from this model showed that the kinematic coupling ratio of 90% is associated with lithospheric stresses at the PAC – BAJA plate boundary, on the order of 10 MPa. Simultaneous coupling stresses between BAJA and NAM (Gulf of

California) need to be low in order to allow BAJA to move as a rigid microplate (Appendix B).

The velocity of BAJA is balanced by the driving forces (coupling stresses along BAJA – PAC plate boundary) and the resisting forces in western NAM. The present-day resisting forces include the dynamics related to deformation around the San Andreas Fault restraining bend, fault slip at the Eastern California Shear Zone, and possibly the motion of the Sierra Nevada (SIERRA) microplate (Plattner et al., 2009; see here chapter 3). Considering that the formation of fault zones in western NAM lowered the resisting forces during the last 3 Myrs, it could be concluded that higher coupling stresses were necessary in the past for keeping plate motions between PAC – BAJA and BAJA – NAM constant. As the coupling was explained by buoyancy of young oceanic slabs subducted under BAJA (Nicholson et al., 1994), it is speculated that the decrease in coupling is due to slab cooling, which caused a decrease in buoyancy (see Appendix B).

In chapter 3 (Plattner et al., 2009) it has been shown that SIERRA microplate motion could be entirely explained as a dynamic response to BAJA motion, without the necessity of other driving forces within SIERRA. Additional numerical modeling (Plattner et al., submitted; see here chapter 4) showed that shear strain in western NAM resulting from BAJA motion could also explain the formation of the eastern SIERRA microplate boundary, the Eastern California Shear Zone. This result support the idea of northward propagation of the Gulf of California fault system, i.e. eastward and inland migration of the major PAC – NAM plate boundary (Faulds et al., 2005). On the other hand, it was shown that the ECSZ can have formed in response to driving forces along the SIERRA - PAC plate boundary (SAF) in combination

with pre-existing weakness in the Basin and Range. As driving forces for SIERRA could have occurred prior to 6 Ma, this scenario agrees better with results from geological studies on the initiation of strike-slip faulting in the northern ECSZ (McQuarrie and Wernicke, 2005). Therefore the hypothesis of the ECSZ having formed from SIERRA motion cannot be rejected. In any case, the northward motion of BAJA, starting at 6 Ma, would have intensified shear strain accommodation and accelerated fault slip rates along the ECSZ (Plattner et al., submitted, see here chapter 4).

Overall, it was found that microplates could be externally driven, by coupling in the lithosphere to their large neighboring plates along the common plates boundaries. Externally driven microplate influence adjacent microplates and smaller blocks in their kinematics and play an important role in the plate boundary evolution. The motion of microplates can lead to the formation of large shear zones, with the shear zone formation being strongly influenced by the presence of pre-existing weakness in the lithosphere. Studying the dynamics in diffuse plate boundaries, it is therefore extremely important to consider the interaction of these multiple rigid blocks.

## 6. References

- Allan, C. R., Silver, L., and Stehli, F.G., 1960, Agua Blance fault, a major transverse structure of northern Baja California, Mexico, *Geol. Soc. Am. Bull.*, 71, 457-482.
- Argus, D.F. and Heflin, M.B., 1995, Plate motion and crustal deformation estimated with geodetic data from the Global Positioning System, *Geophys. Res. Lett.*, 22, 1973-1976.
- Atwater, T., and Stock, J.M., 1998, Pacific-North America plate tectonics of the Neogene Southwestern United States: An Update, *Int. Geol. Rev.*, v. 40, no. 5, p. 375-402.
- Atwater, T. and Stock, J., 1988, Pacific – North America Plate Tectonics of the Neogene Southwestern United States – An Update, in Ernst, W.G. & Nelson, C.A., eds., *Integrated Earth and environmental evolution of the southwestern United States: The Clarence A. Hall, Jr. volume:* Columbia, Bellwether Publishing, 393-420.
- Becker, T.W., Hardebeck, J.L., and Anderson, G., 2005, Constraints on fault slip rates of the southern California plate boundary from GPS velocity and stress inversions: *Geophysical Journal International*, v. 160, p. 634–650, doi: 10.1111/j.1365-246X.2004.02528.x.
- Beavan, J., Tregoning, P., Bevis, M., Kato, T. and Meertens, C., 2002, Motion and rigidity of the Pacific Plate and implications for plate boundary deformations, *J. Geophys. Res.*, 107, 2261, doi:10.1029/2001JB000282.
- Busch, M.M., Arrowsmith, J.R., Gutierrez, G.M., Toke, N., Brothers, D.,

- Dimaggio, E., Maloney, S., Zileke, O., and Buchanan, B., 2006, Late Quaternary faulting in the Cabo San Lucas-La Paz Region, Baja California. *Eos Trans. AGU*, 87(52), Fall Meet. Suppl., Abstract T41D-1612.
- DeMets, C., 1995, A reappraisal of seafloor spreading lineations in the Gulf of California: Implications for the transfer of Baja California to the Pacific plate and estimates of Pacific-North America motion, *Geophys. Res. Lett.*, 22, 3545-3548.
- DeMets, C., Gordon, R.G., Argus, D.F. and Stein, S., 1990, Current plate motions, *Geophys. J. Int.*, 101, 425-478.
- DeMets, C., Gordon, R.G., Argus, D.F. and Stein, S., 1994, Effect of Recent Revisions to the Geomagnetic Reversal Time-Scale on Estimates of Current Plate Motions, *Geophys. Res. Lett.*, 21, 2191.
- DeMets, C. and Dixon, T.H., 1999, New kinematic models for Pacific-North America motion from 3 Ma to present, I: Evidence for steady motion and biases in the NUVEL-1A model, *Geophys. Res. Lett.*, 26, 1921-1924.
- Dixon, T.H., 1991, An introduction to the Global Positioning System and some geological applications, *Reviews of Geophysics*, v.29, 249-276.
- Dixon, T.H., Miller, M., Farina, F., Wang, H. and Johnson, D., 2000a, Present day motion of the Sierra Nevada block and some implications for the Basin and Range province, North America Cordillera, *Tectonics*, 19, 1-24.
- Dixon, T.H., Farina, F., DeMets, C., Suarez-Vidal, F., Fletcher, J., Marquez-Azua, B., Miller, M., Sanchez, O. and Umhoefer, P., 2000b, New

Kinematics for Pacific-North America Motion from 3 Ma to present, II: Evidence for a "Baja California shear zone", *Geophys. Res. Lett.*, 27, 3961-3964.

Dixon, T.H., Decaix, J., Farina, F., Furlong, K., Malservisi, R., Benett, R., Suarez-Vidal, F., Fletcher, J. and Lee, J., 2002, Seismic cycle and rheological effects on estimation of present-day slip rates for the Agua Blanca and San Miguel-Vallecitos faults, northern Baja California, Mexico, *J. Geophys. Res.*, 107, doi:10.1029/2000JB000099.

Dokka, R.K., Travis, C.J., 1990, Role of the Eastern California shear zone in accommodating Pacific-North America plate motion, *Geophys. Res. Lett.*, v. 17, no. 9, p. 1323-1326.

Faulds, J.E., Henry, C.D., and Hinz, N.H., 2005a, Kinematics of the northern Walker Lane: An incipient transform fault along the Pacific - North American plate boundary: *Geology*, v. 33, no. 6, p. 505-508.

Faulds, J.E., Henry, C.D., Hinz, N.H., Drakos, P.S., Delwiche, B., 2005b, Transect across the Northern Walker Lane, northwest Nevada and northeast California: an incipient transform fault along the Pacific-North America plate boundary, in Pederson, J., Dehler, C.M., eds, *Interior Western United States, Geol. Soc. Am. Field Guide 6*, p.129-150, doi:10.1130/2005.fld006(06).

Flesch, L., Holt, W.E., Haines, A.J., Shen-Tu, B., 2000, Dynamics of the Pacific-North American Plate Boundary in the Western United States, *Science*, v. 287, 5454, pp.834-836, doi: 10.1126/science.287.5454.834.

Fletcher, J.M. and Munguia, L., 2000, Active continental rifting in southern Baja California, Mexico: Implications for plate motion partitioning and

the transition to seafloor spreading in the Gulf of California, *Tectonics*, 19, 1107-1123.

Fletcher, J.M., Grove, M., Kimbrough, D., Lovera, O., and Gehrels, G.E., 2007, Ridge-trench interactions and the Neogene tectonic evolution of the Magdalena shelf and southern Gulf of California: Insights from detrital zircon U-Pb ages from the Magdalena fan and adjacent areas: *Geological Society of America Bulletin*, v. 119, p. 1313-1336.

Forsyth, D., and Uyeda, S., 1975, On the relative importance of the driving forces of plate motion, *Geophys. J. R. astr. Soc.*, 43, 163-200.

Freymueller, J.T., Murray, M.H., Segall, P. and Castillo, D., 1999, Kinematics of the Pacific - North America plate boundary zone, northern California, *J. Geophys. Res.*, 104, 7419-7441.

Gardi, A., Sabadini, R., Ferraro, C., and Aoudia, A., 2003, The interplay between global tectonic processes and the seismic cycle in the Umbria-Marche seismogenic region: *Geophysical Journal International*, v. 155, p. 1093–1104, doi: 10.1111/j.1365-246X.2003.02117.x.

Gastil, R.G., Phillips, P.R. and Allison, C.E., 1975, Reconnaissance Geology of the State of Baja California, *Geol. Soc. Am. Mem.*, 140, 170p

Gonzales-Garcia, J.J., Prawirodirdjo, L., Bock, Y. and Agnew, D., 2003, Guadalupe Island, Mexico as a new constraint for Pacific plate motion, *Geophys. Res. Lett.*, 30(16), 1872, doi:10.1029/2003GL017732.

Govers, R., and Meijer, P.T., 2001, On the dynamics of the Juan de Fuca plate: *Earth and Planetary Science Letters*, v. 189, p. 115–131, doi: 10.1016/S0012-821X(01)00360-0.



- Govers, R. and Wortel, M.-J.-R., 2005, Lithosphere tearing at STEP faults: response to edges of subduction zones, *Earth Planet. Sc. Lett.*, 236, 1-2, 505-523.
- Harry, D.L., 2005, Evolution of the western U.S. Walker Lane and East California shear zone: insights from geodynamic modeling, *Geol. Soc. Am Abstract with Programs*, v. 37, no. 7, p.59.
- Hausback, B.P., 1984, Cenozoic volcanic and tectonic evolution of Baja California Sur, Mexico, in *Geology of the Baja Peninsula*, vol. 39, edited by Frizell, V.A., pp. 219-236, *Pac. Sect. Soc. of Econ. Paleontol. and Mineral.*, Los Angeles, Calif.
- Hough, S.E., Hutton, K., 2008, Revisiting the 1872 Owens Valley, CA, Earthquake, *Bull. Seis. Soc. Am.*, v. 98, no. 2 p. 931-949, doi: 10.1785/0120070186.
- Iaffaldano, G., and Bunge, H.-P., 2008, Strong plate coupling along the Nazca/South America convergent margin: *Geology*, v. 36, p. 443–446, doi: 10.1130/G24489A.1.
- Jennings, C.W., 1994, *Fault Activity Map of California and Adjacent Areas: Sacramento, CA, USA*, Dept. of Conservation, division of Mine and Geology.
- Kearey, P., Klepeis, K.A., Vine, F.J., 2009, *Global Tectonics*, 3rd editions, Wiley Blackwell, Chichester, UK isbn 978-1-4051-0777-8.
- Kohlstedt, D.L., Evans, B., and Mackwell, S.J., 1995, Strength of the Lithosphere - Constraints Imposed by Laboratory Experiments: *Journal of Geophysical Research*, v. 100, p. 17587–17602, doi: 10.1029/95JB01460.

- Kumar, R.R., Gordon, R.G. and Landis, C.M., 2006, Horizontal thermal contractional strain of oceanic lithosphere: The ultimate limit to the rigid plate hypothesis, *Eos Trans. AGU*,87(52), Fall Meet. Suppl., Abstract G41A-04.
- Lachenbruch, A., and Sass, J., 1980, Heat flow and energetics of the San Andreas fault zone: *Journal of Geophysical Research*,v.85,p.6185–6222.
- Lachenbruch, A.H., Sass, J.H., and Galanis, S.P., Jr., 1985, Heat Flow in Southernmost California and the Origin of the Salton Trough, *J. Geophys. Res.*, 90, 6709-6736.
- Lachenbruch, A., and Sass, J., 1992, Heat flow from Cajon Pass, fault strength, and tectonic implications: *Journal of Geophysical Research*, v.97, p.4995–5015.
- Lambeck, K., 1988, *Geophysical geodesy: the slow deformations of the Earth*: New York, USA, Oxford University Press.
- Larson, K.M., Freymueller, J.T. and Philipson, S., 1997, Global plate velocities from the Global Positioning System, *J. Geophys. Res.*, 102, 9962-9982.
- Legg, M.R., Wong, V.O. and Suarez-Vidal, F., 1991, Geologic structure and tectonics of the inner continental borderland of northern Baja California, in J. Dauphin and B. Simoneit, eds., *Gulf and Peninsular Province of the Californias*, *Am. Assoc. Pet. Geol. Mem.* 47, 145-177.
- Li, Q., Liu, M., 2006, Geometrical impact of the San Andreas fault on stress and seismicity in California, *Geophys. Res. Lett.*, v. 33, L08302.
- Lonsdale, P., 1989, *Geology and tectonic history of the Gulf of California*, *in*

Winterer, E.L., Hussong, D.M., and Decker, R.W., eds., The eastern Pacific Ocean and Hawaii, Volume N: The geology of North America: Denver, CO, USA, Geol. Soc. Am., 499–521.

Lonsdale, P., 1991, Structural patterns of the Pacific floor offshore of Peninsular California, *in* Dauphin, J.P., and Simoneit, B.R.T., eds., The Gulf and Peninsular Province of Californias, Volume 47: AAPG Memoir, Ocean Drilling Program, 87–125.

Mao, A., Harrison, G.A. and Dixon, T.H., 1999, Noise in GPS coordinate time series, *J. Geophys. Res.*, 104, 2797-2816.

McCaffrey, R., 2002, Crustal block rotations and plate coupling, in S. Stein and J. Freymueller, eds., Plate Boundary Zones, *Geodyn. Ser.*, vol. 30, edited by, pp.101-122.

McCrary, P.A., Wilson, D.S., Stanley, R.G., 2009, Continuing evolution of the Pacific-Juan de Fuca-North America slab window system- A trench-ridge-transform example from the Pacific Rim, *Tectonophysics*, v. 464, p. 30-42, doi:10.1016/j.tecto.2008.01.018.

McQuarrie, N. and Wernicke, B.P., 2005, An animated tectonic reconstruction of southwestern North America since 36 Ma. *Geosphere*, 1, 3, doi: 10.1130/GES00016.1, 147-172.

Melosh, H.J., and Williams, C.A., 1989, Mechanics of Graben Formation in Crustal Rocks - a Finite-Element Analysis: *Journal of Geophysical Research*, v. 94, p. 13961–13973, doi: 10.1029/JB094iB10p13961.

Michaud, F., Sosson, M., Royer, J.Y., Chabert, A., Bourgois, J., Calmus, T., Mortera, C., Bigot-Cormier, F., Bandy, W., Dymant, J., Pontoise, B., and Sichler, B., 2004, Motion partitioning between the Pacific plate,

Baja California and the North America plate: The Tosco-Abreojos fault revisited: *Geophysical Research Letters*, v. 31, doi: 10.1029/2004GL019665.

Michaud, F., Royer, J.Y., Bourgois, J., Dymant, J., Calmus, T., Bandy, W., Sosson, M., Mortera-Gutiérrez, C., Sichler, B., Rebolledo-Viera, M., and B. Pontoise, 2006, Oceanic-ridge subduction vs. slab break off: Plate tectonic evolution along the Baja California Sur continental margin since 15 Ma: *Geology*, v. 34, p.13-16, doi: 10.1130/g22050.1.

Miller, D.M., and Yount, J.C., 2002, Late Cenozoic tectonic evolution of the north-central Mojave Desert inferred from fault history and physiographic evolution of the Fort Irwin area, California, in Glazner, A.F., Walker, J.D., and Bartley, J.M., eds., *Geologic Evolution of the Mojave Desert and Southwestern Basin and Range, Volume 195: Geological Society of America Memoir: Boulder, CO, Geological Society of America*, p. 173-197.

Minster, J.B., Jordon, T.H., Molnar, P. and Haines, E., 1974, Numerical Modelling of Instantaneous Plate Tectonics. *Geophys. J. R. astr. Soc.*, 36, 541-576.

Nicholson, C., Sorlien, C.C., Atwater, T., Crowell, J.C. and Luyendyk, B.P., 1994, Microplate capture, rotation of the western Transverse Ranges, and initiation of the San Andreas transform as a low-angle fault system. *Geology*, 22, 491-195.

Oskin, M. and Iriondo, A., 2004, Large-magnitude transient strain accumulation on the Blackwater fault, Eastern California shear zone, *Geology*, v. 32, p. 313-316, doi: 10.1130/G20223.1

- Plattner, C., Malservisi, R., Dixon, T.H., LaFemina, P., Sella, G.F., Fletcher, J., and Suarez-Vidal, F., 2007, New constraints on relative motion between the Pacific Plate and Baja California microplate (Mexico) from GPS measurements: *Geophysical Journal International*, v. 170, p. 1373-1380.
- Plattner, C., Malservisi, R., Govers, R., 2009, On the plate boundary forces that drive and resist Baja California motion, *Geology*, v. 37, p. 359–362, doi:10.1130/G25360A.1
- Plattner, C., Malservisi, R., Furlong, K., Govers, R. , Development of the Eastern California Shear Zone: Effect of pre-existing weakness in the Basin and Range? (submitted to *Tectonophysics*).
- Psencik, K.O., Dixon, T.H., Schmalzle, G., McQuarrie, N., and McCaffrey, R., 2006, Improved present day euler Vector for Sierra Nevada block using GPS: *EOS Trans. AGU, Fall Meet. Suppl.*, Abstract G42A–04.
- Ray, J., Dong, D. and Altamimi, Z., 2004, IGS reference frames: status and future improvements, *GPS Solutions*, 8, 251-266.
- Reheis, M. C., and Sawyer, T.L. 1997, Late Cenozoic history and slip rates of the Fish Lake Valley, Emigrant Peak, and Deep Springs fault zones, Nevada and California, *Bull. Geol. Soc. Am.*, 109, 280 – 299.
- Sandwell, D., Sicho, L., Agnew, D., Bock, Y., Minster, J-B., 2000, Near real-time radar interferometry of the Mw 7.1 Hector Mine Earthquake, *Geophys. Res. Lett.*, v. 27, no. 9, p.3101-3104.
- Sella, G.F., Dixon, T.H. and Mao, A.L., 2002, REVEL: A model for Recent plate velocities from space geodesy, *J. Geophys. Res.*, 107, doi:10.1029/2000JB000033.

- Sella, G.F., Stein, S., Dixon, T.H., Craymer, M., James, T.S., Mazzotti, S. and Dokka, R.K., 2006, Observation of Glacial Isostatic Adjustment in "Stable" North America with GPS, *Geophys. Res. Lett.*, 34, L02306, doi: 10.1029/2006GL027081.
- Spencer, J.-E. and Normark, W., 1979, Tosco-Abreojos fault zone: A Neogene transform plate boundary within the Pacific margin of southern Baja California, Mexico, *Geology*, 7, 554-557.
- Stein, S. and Gordon, R.G., 1984, Statistical tests of additional plate boundaries from plate motion inversions. *Earth Plan. Sci. Lett.*, 69, 2, 401-412.
- Stock, J.M., and Hodges, K.V., 1989, Pre-Pliocene extension around the Gulf of California and the transfer of Baja California to the Pacific Plate. *Tectonics*, 8, 99-115.
- Stock, J. M., and Lee, J., 1994, Do microplates in subduction zones leave a geological record? *Tectonics*, 13(6), 1472-1487, 10.1029/94TC01808.
- Stüwe, K., 2007, *Geodynamics of the Lithosphere*: Berlin, Springer, 493 pp.
- Suarez-Vidal, F., Armijo, R., Morgan, G., Bodin, P. and Gastil, R.G., 1991, Framework of recent and active faulting in Northern Baja California; in J. Dauphin and B. Simoneit, eds., *Gulf and Peninsular Province of the Californias*, *Am. Assoc. Pet. Geol. Mem.* 47, 285-300.
- Thatcher, W., 1995, Microplate versus continuum descriptions, *J. Geophys. Res.*, 100, 3885-3894.
- Umhoefer, P.J., 2000, Where are the missing faults in translated terranes?: *Tectonophysics*, 326, 23-35.

- Umhoefer, P.J., and Dorsey, R.J., 1997, Translation of terranes; lessons from central Baja California, Mexico, *Geology*, 25, 1007-1010.
- Umhoefer, P.J., 2007, Late quaternary faulting along the San Juan de los Planes fault Zone, Baja California Sur, Mexico, *Eos Trans. AGU*, 88(52), Fall Meet. Suppl., Abstract T41A-0357.
- Unruh, J., Humphrey, J., and Barron, A., 2003, Transtensional model for the Sierra Nevada frontal fault system, eastern California: *Geology*, v. 31, p. 327–330, doi: 10.1130/0091-7613(2003)031<0327:TMFTSN>2.0.CO;2.
- Ward, S., 1990, Pacific-North America Plate Motions: New Results From Very Long Baseline Interferometry, *J. Geophys. Res.*, 95, 21965-21981.
- Wesnousky, S.G., 2005, The San Andreas and Walker Lane fault systems, western North America: transpression, transtension, cumulative slip and the structural evolution of a major transform plate boundary: *Journal of Structural Geology*, v. 27, p. 1505–1512, doi: 10.1016/j.jsg.2005.01.015.
- Zhang, X., Paulssen, H., Lebedev, S., and Meier, T., 2007, Surface wave tomography of the Gulf of California: *Geophysical Research Letters*, v. 34, doi: 10.1029/2007gl030631.
- Zumberge, J.F., Heflin, M.B., Jefferson, D.J., Watkins, M.M. and Webb, F.H., 1997, Precise point positioning for the efficient and robust analysis of GPS data from large networks, *J. Geophys. Res.*, 102, 5005-5017.

## 7. Appendix A: Preliminary velocity field in central BAJA

The accommodation of the residual motion within BAJA, as seen from the contraction between the northern and southern GPS network with a strain rate of  $10^{-16} \text{ s}^{-1}$  remains unclear. Preliminary velocity data from central BAJA (with currently only two positioning observations in the time-series) do not allow distinguishing between diffuse deformation and the presence of an unrecognized fault structure between northern and southern BAJA.

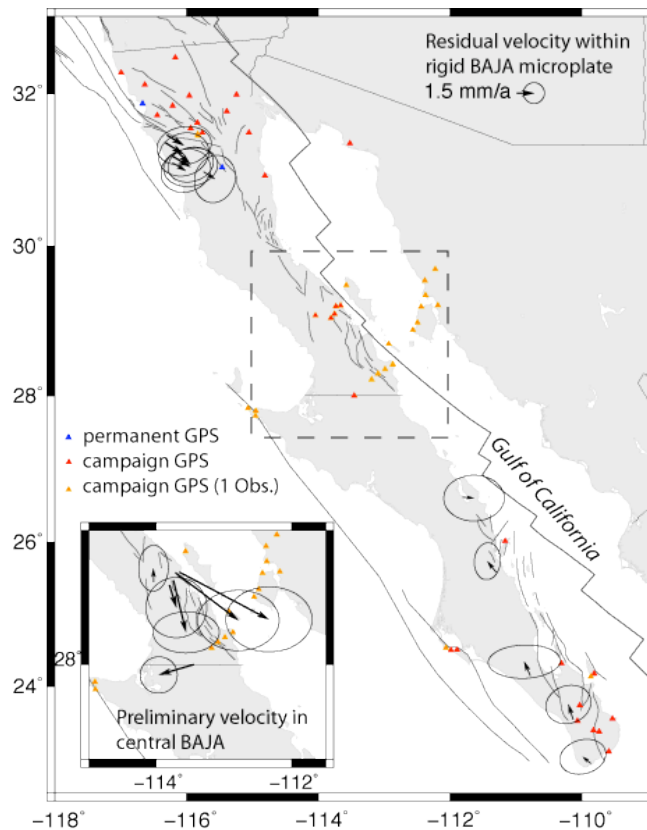


Figure A.1: Residual velocities in rigid BAJA (see Figure 2.4). Preliminary velocities in central BAJA show that stations inside the microplate are within uncertainty, compatible with the computed rigid motion of BAJA. Velocities from stations in the east show strain accumulation from the nearby faults.



## 8. Appendix B: Coupling stresses at the PAC - BAJA plate boundary

### B.1 Plate motion partitioning across NAM – PAC in dependency on the stress magnitude

If no shear stress is applied along the PAC – BAJA plate boundary (SBTA fault), the fault velocity at this plate boundary hosts about the same relative motion than NAM – BAJA. Increasing the differential shear stress along PAC-BAJA from zero, the velocity at PAC – BAJA decreases, and increases the velocity along the NAM – BAJA plate boundary (Gulf of California). The coupling stresses can be increased until BAJA becomes part of the PAC plate. At this point, the full NAM – PAC plate boundary will be accommodated in the Gulf of California. The geodetic relative motions across this plate boundary agree with the modeled partitioning for a shear stress of 10 MPa.

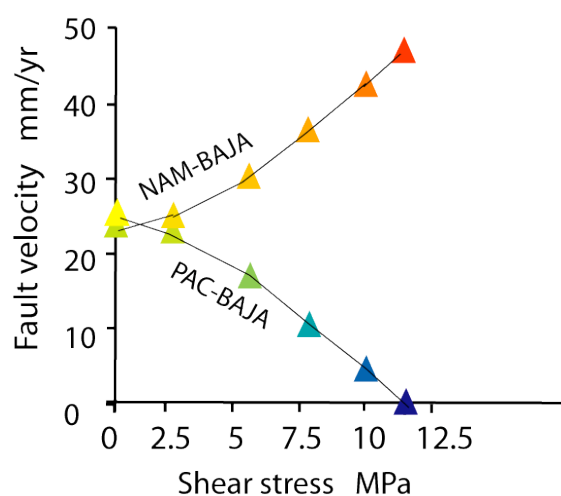


Figure B.1: Fault velocity at the NAM – BAJA and PAC-BAJA plate boundary for different differential shear stress applied at the PAC-BAJA plate boundary.

## **B.2 Influence of incomplete decoupling in the Gulf of California**

The partitioning of relative motion, and the necessary shear stress applied to the PAC – BAJA plate boundary for reproducing the geodetic relative plate motions depend on the resisting forces for BAJA motion in western NAM and along the NAM – BAJA plate boundary (Gulf of California). In chapter 3 it was assumed that the Gulf of California is a boundary between two completely decoupled plates. Before the rupture of BAJA from NAM, during the Protogulf extension, this was not true and also the current state is incompletely known. The presence of such coupling stresses in the Gulf of California decreases the relative motion of BAJA with respect to NAM. To still fit the geodetic BAJA motions, the stresses along the PAC – BAJA plate boundary need to be increased by the same amount as stresses in the Gulf of California are, in order balance the driving and resisting forces, keeping the velocity constant. However, for coupling stresses in the Gulf of California approaching 5 MPa or more, the relative motion of BAJA with respect to the PAC and NAM plate is not accommodated anymore by localized fault slip, but by continuum deformation over a broader region. Kinematic results suggested rigidity of BAJA, and therefore low coupling stresses in the Gulf of California. For the time during the Protogulf extension it has to be assumed that deformation was localized along the weak former volcanic, allowing BAJA to remain undeformed.

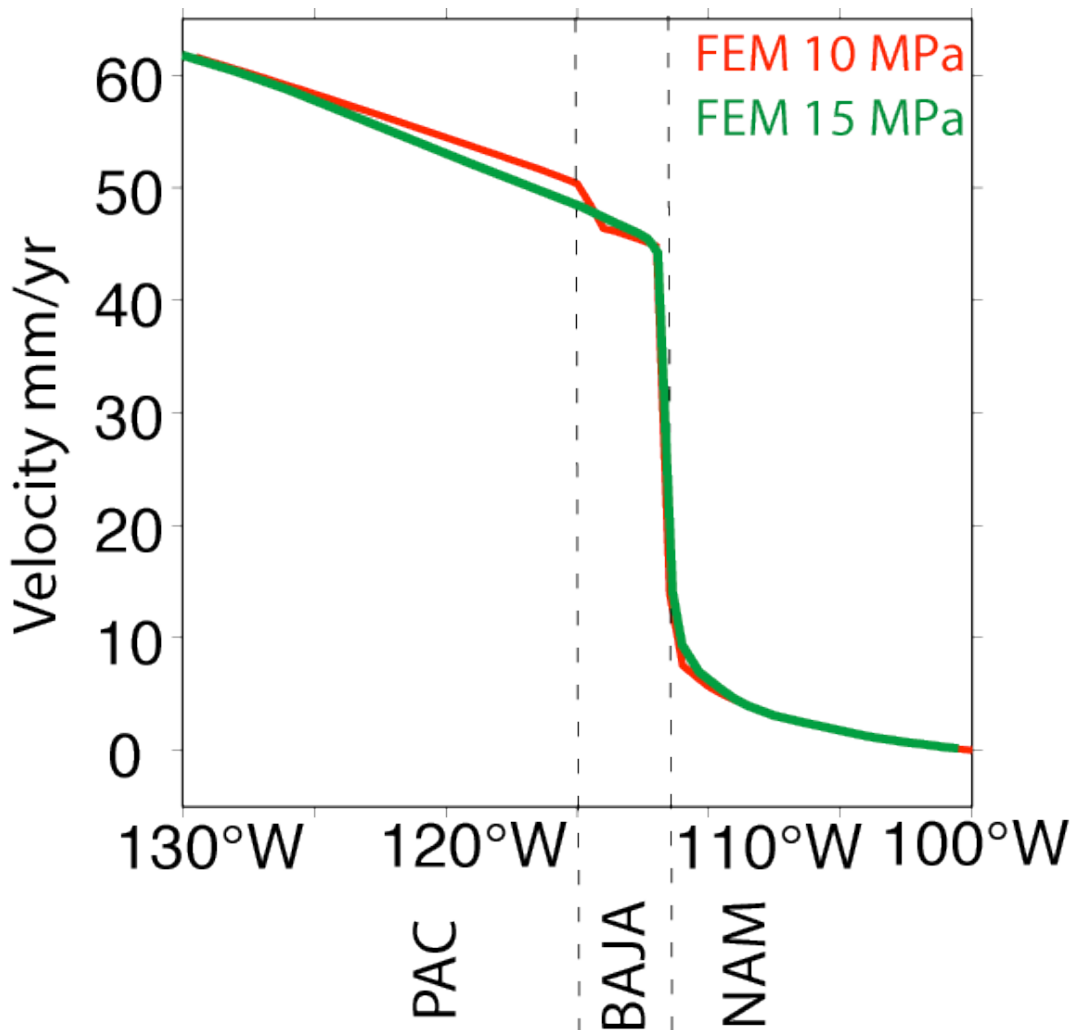


Figure B.2: Velocity profile across latitude 28°N. Red line: results from a model in which the plate boundary in the Gulf of California is stress-free. Green line: results from a model with 5 MPa coupling stresses in the Gulf of California. The necessary coupling stresses along the PAC – BAJA plate boundary (see upper right corner) has to be increased by the coupling stresses in the Gulf of California for reproducing the present-day velocity of BAJA with respect to the North American plate. High stresses across the PAC – BAJA plate boundary lead to continuum deformation rather than localized fault slip.

### **B.3 Temporal evolution of PAC – BAJA coupling**

Since the western NAM imposes resisting forces for BAJA motion, the formation of new fault zones since 6 Ma implies a decrease of these resisting forces. It is known that the southern Eastern California Shear Zone has formed after 4 Ma, and the San Jacinto Fault and Elsinore Fault around 2 Ma. For constant coupling stresses along the PAC – BAJA plate boundary our model shows a decrease of BAJA motion with respect to NAM if these faults are not included. However, comparison of geodetic and geologic plate relative motions suggested constant velocities during the last 3 Myrs between BAJA and NAM (Figure 2.7). In this case, the coupling stresses would have needed to be higher in the past than today. A possible explanation for decreasing coupling is cooling of stalled slabs associated to decreasing buoyancy. Such process would then be expected to have started not only 3 Ma, but have initiated after the cessation of seafloor spreading and subduction at 12 Ma.



# CURRICULUM VITAE

## Personal information

---

Name: Christina Plattner  
Address: Schüsselkarstr. 3, 82377 München, Germany  
Telephone: 0049.89.7142753, 0049.178.8786356  
Email: plattner@geophysik.uni-muenchen.de  
Date and place of birth: 08.06.1979, Munich, Germany  
Nationality: German

## Education and Study

---

Since August 2005 *Doctoral thesis* "Implications of Baja California microplate motion on the North America – Pacific plate boundary region", DFG funded project and within the international graduate school THESIS of the Elitenetzwerk Bayern, Section Geophysics, Ludwig-Maximilians Universität (LMU) München, Germany.

1999 – 2005 *Diploma study of Geography, Geology, and Geophysics* at LMU, passed with distinction (1,1). Diploma thesis with the Commission for Glaciology, Bavarian Academy of Sciences: „The spatial variation of snow accumulation at Vernagtferner in the Austrian Alps in winter 2003/2004“.

1999 Graduation for University entrance, Neuhofer Gymnasium München, Germany.

## Publications

---

Plattner, C., Malservisi, R., Furlong, K., and Govers, R (submitted to Tectonophysics). Strain accumulation along the Eastern California Shear Zone – Walker Lane belt. Effect of preexisting weakness in the Basin and Range?

Plattner, C., Malservisi, R. and Govers, R, (2009). On the plate boundary forces that drive and resist Baja California, *Geology*, v. 37, p. 359 – 262, doi:

10.1130/G25360A.1

Plattner, C., Malservisi R., Dixon T.H., LaFemina P., Sella G., Fletcher J., Suarez-Vidal F., (2007). New constraints on relative motion between the Pacific plate and Baja California microplate (Mexico) from GPS measurements. *Geophysical Journal International*, doi:10.1111/j.1365-246X.2007.03494.x

Plattner, C., Braun, L. and Brenning, A., (2006). The spatial variability of snow accumulation at Vernagtferner, Austrian Alps, in winter 2003/2004. *Zeitschrift fuer Gletscherkunde und Glazialgeologie*, B39-2003/2004, 43-57.

#### Conference contributions

---

##### Oral presentations:

American Geophysical Union (AGU) Fall Meeting 2008; European Geoscience Union General Assembly 2008 and 2007; Alpine Glaciological Meeting (AGM) 2005.

##### Poster presentations:

AGU Fall Meeting 2008, 2007, 2006, and 2005; EGU General Assembly 2006 and 2007; MARGINS Rupture Continental Lithosphere Cortez Workshop 2006; AGM 2006.

#### Awards and Memberships

---

01/2009 AGU Fall Meeting 2008 Outstanding Student Paper Award (Tectonophysics section).

11/2007 acceptance into the LMU Mentoring-Programme in the framework of LMUexcellent. Supervision Prof. B. Reichenbacher (LMU), Dr. O. Heidbach (GFZ Potsdam).

12/2005 MARGINS Student Prize (Honorable Mention) for AGU Fall Meeting contribution.

11/2005 acceptance into the international graduate school THESIS of the Elitenetzwerk Bayern.

Professional Societies AGU, EGU